DSPACE

https://dspace.org/

The Influence of Footwall Rock Materials on the Rock Mass Response to Seismicity at Mponeng Gold Mine

Nkomo, Darlington Brilliant

2025
University of the Witwatersrand, Johannesburg
https://hdl.handle.net/10539/49829

Nkomo, Darlington Brilliant. (2025). The Influence of Footwall Rock Materials on the Rock Mass Response to Seismicity at Mponeng Gold Mine. [Master's dissertation, University of the Witwatersrand, Johannesburg]. WIReDSpace. https://hdl.handle.net/10539/49829

Downloaded from a DSpace repository. https://dspace.org/

School of Mining Engineering



UNIVERSITY OF THE
WITWATERSRAND,
JOHANNESBURG

THE INFLUENCE OF FOOTWALL ROCK MATERIALS ON THE ROCK MASS RESPONSE TO SEISMICITY AT MPONENG GOLD MINE

Darlington Brilliant Nkomo

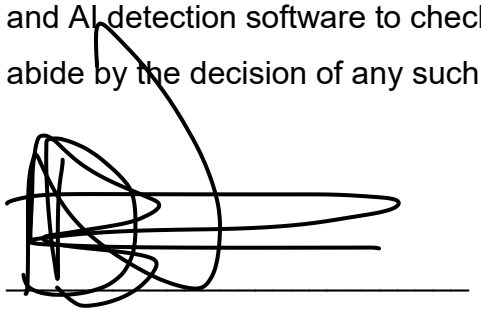
Student Number: 0713948A

I declare that this research report is my own unaided work. It is being submitted for the degree of Master of Science at the University of the Witwatersrand, Johannesburg. It has not been submitted before for any degree or examination to any other university.

Johannesburg, 2025

DECLARATION

I have familiarised myself with the University of the Witwatersrand Student Academic Misconduct Policy (SAMP). I hereby declare that the work I am submitting for assessment is my original work. I affirm that I have not plagiarised, misrepresented, or colluded with any other person or source. I have properly acknowledged, cited, and referenced all the sources that I have used in my work. I also declare that I have used artificial intelligence (AI) tools only as a means of guidance. The ideas and arguments presented in my work are my original thoughts and interpretations. I acknowledge that any academic misconduct, such as plagiarism or collusion, will result in serious consequences. These consequences may include a reduced grade, a fail mark, or disciplinary action according to the SAMP. The School of Mining Engineering has my consent to investigate any potential academic misconduct in my work. This investigation may include the use of similarity and AI detection software to check the originality of my work. I undertake to abide by the decision of any such investigation.



Signature of Candidate

___4th____ day of ___September_____, __2025_____

“*Keep your face always toward the sunshine - and shadows will fall behind you.”*

Walt Whitman

ABSTRACT

Mponeng Mine is currently the deepest mine in the world, mining at a depth of 3500 m below the surface. The active mining stopes are in a very high-stress environment, and the mine is highly seismically active. Seismicity has been the main driver of the fall of ground incidents recorded at the Mponeng Mine over the years. The seismically induced falls of ground have contributed to multiple fatal accidents and loss of production. Between 2013 and 2023, there were 315 seismic-related accidents, of which 13 resulted in fatalities. Of the 13 fatalities, 12 were in the stopes and one was in an off-reef development excavation. There are two footwall zones at the mine: quartzite on the west and shale to the east. Of the 12 fatalities in the stopes, 8 were in the quartzite footwall zone and 4 in the shale footwall zone. Some conclusions were drawn following laboratory strength analyses of the two different footwall rock types at Mponeng Mine. The mechanical properties of the lava hanging wall are almost constant throughout the mine. However, the footwall rock types are different. The mechanical properties vary significantly between the quartzite and shale footwalls. In particular, the quartzite footwall is significantly more brittle than the shale. The different footwall properties play a role in the stress distribution around the stopes, which influences the ground conditions of the hangingwall and footwall. The hangingwall above in the quartzite footwall was significantly more fractured than in the areas with a shale footwall. The quartzite footwall was also highly fractured and undulating. At the current depth of mining, the hangingwall was expected to be highly fractured, except where the face was de-stressed by pre-conditioning or over-stoping. Preconditioning in both footwall zones was done properly, but the deeper fracture distance in the shale footwall contributed to a better ground condition. The quartzite footwall zone generated a high number of small magnitude events ahead of the face with higher damaged volume, while the shale footwall zone generated a high number of larger magnitude events with far less damage. However, Map3D elastic numerical modelling software showed a higher energy release rate in the shale area. The softer Booysen's shale appears to absorb more strain energy during static and dynamic loading than the quartzite zones. The shale is also more prone to creep, allowing closure and reducing fracturing in the hangingwall. The quartzite material fractures more easily, generating smaller magnitude events. The highly fractured rock in the quartzite zone suffers greater shakedown damage during the vibrations caused by a seismic event. Based on the findings of this research, the support resistance in

Booysen’s shale footwall stopes may be lower and the extraction ratio higher than in areas with a quartzite footwall.

ACKNOWLEDGMENTS

Firstly, I would like to thank God for guiding me through the process. Words cannot express my gratitude to Professor Bryan Watson for his invaluable patience and feedback. Also, I could not have undertaken this journey without the Mponeng Management and Rock Engineering team, who allowed me to use their data and generously provided information when requested. Many thanks to Dr. Halil Yilmaz, who assisted with the laboratory tests of the intact rock samples. Additionally, this endeavour would not have been possible without the generous support from the Dwarsrivier Chrome Mine for affording me the time to complete this study.

Secondly, I would like to thank Thelma Boke for going out of her way to ensure that I get the Map3D license and dongle to assist with the data analysis. Her efforts are greatly appreciated.

Lastly, I would be remiss in not mentioning my family, especially my spouse and children. Their belief in me has kept my spirits and motivation high during this process. Their patience and understanding during the late nights and indoor weekends are greatly appreciated. The prayers from my family and the constant encouragement are highly appreciated.

TABLE OF CONTENTS

DECLARATION i

ABSTRACT iii

ACKNOWLEDGMENTS v

LIST OF FIGURES x

LIST OF TABLES xiii

APPENDIX LIST OF TABLES xiii

LIST OF EQUATIONS xiii

LIST OF ABBREVIATIONS AND SYMBOLS xiv

1 INTRODUCTION 1

1.1 Research Background and Context 2

1.2 Problem Statement 3

1.3 Justification for Research 4

1.4 Research Objectives 4

1.5 Research Methods 4

1.6 Source of Data 6

1.7 Research Validation 6

1.8 Structure of the Research Report 6

2 LITERATURE REVIEW 8

2.1 Introduction 8

2.2 Key Concepts, Theories and Studies 8

2.2.1 The Ventersdorp Contact Reef 8

2.2.2 Lithology of the VCR 9

2.2.3 Mining sequence and support strategy 14
2.2.4 Seismicity and Rockburst 16
2.2.5 Seismic event sources 17
2.2.6 Energy Release Rate 19
2.2.7 Intact rock strength 20
2.2.8 Rock mass classification 23
2.2.9 Rock mass strength 24
2.2.10 Influence of rock strength on ground conditions 25
2.3 Key Debates and Controversies 25
2.4 Chapter Summary 26
3 RESEARCH APPROACH 28
3.1 Introduction 28
3.2 Research Design 28
3.3 Data Collection Process 28
3.3.1 Physical ground conditions 28
3.3.2 Core sampling collection 29
3.3.3 Laboratory tests 29
3.3.4 Seismic data 29
3.3.5 Elastic Modelling 29
3.4 Data Validation Process 29
3.5 Data Analysis Approach 30
3.6 Chapter Summary 30
4 DATA FOR THE STUDY 31
4.1 Introduction 31
4.1.1 Underground observations 31

4.1.1.1 East Mine 33
4.1.1.2 West mine 34
4.2 Mine plan observations 36
4.3 Rock Strength Properties 37
4.3.1 Uniaxial Compressive Strength Results 37
4.3.2 Numerical modelling results 40
4.4 Seismic Response 42
4.4.1 116/65 and 116/35 geological and geometrical comparisons 43
4.4.2 Seismic comparison between 116/65 and 116/35 raise lines 44
4.5 Chapter Summary 46
5 ANALYSIS AND FINDINGS 47
5.1 Mechanical properties of intact rock 47
5.1.1 Intact rock strength 47
5.1.2 Rock mass strength 48
5.2 Seismic response 50
5.3 Ground conditions 54
5.3.1 Stress fracturing 54
5.3.2 Blasting fractures 55
5.4 Chapter Summary 56
6 CONCLUSIONS AND RECOMMENDATIONS 57
6.1 Introduction 57
6.2 Summary of Chapters 57
6.3 Research Observations 59

6.3.1 Initial and complementary studies 59
6.3.2 Key findings and observations 60
6.4 Research Contributions 60
6.5 Research Limitations 61
6.6 Recommendations for Future Research Work 61
REFERENCE LIST 63
APPENDIX A. TABLE OF LABORATORY UNI-COMPRESSIVE STRENGTH WITH MODULUS TESTS RESULT i

LIST OF FIGURES

Figure 1.1: South African map showing the location of Mponeng Mine near Carletonville. 1
Figure 2.1: Stratigraphy of the Witwatersrand Supergroup. 9
Figure 2.2: Idealised VCR stratigraphy showing the UCS of the over- and underlying rocks 10
Figure 2.3: The geotechnical zones of the VCR in the Witwatersrand Basin mines indicate the position of Western Deep Levels mines. 11
Figure 2.4: Photo of an aphanitic lava rock sample from a drill core 12
Figure 2.5: Photo of a porphyritic lava rock sample from a drill core 12
Figure 2.6: Plan of Mponeng mine showing the location of different footwall zones compared to the current and planned mining area as per the LOM business plan 13
Figure 2.7: Flowchart indicating principal steps of support design methodology 16
Figure 2.8: Relationship of brittleness to Young's modulus and Poisson's ratio 23
Figure 2.9: Stress fractures around a deep stope mined in strong, brittle quartzite 25
Figure 4.1: Macro plan view of Mponeng mine showing the position of the visited stopes (120/33, 123/51, 120/66 and 113/67) 32
Figure 4.2: Photos from different stopes showing the generally smooth hangingwall conditions in the east mine stopes ... 34
Figure 4.3: Smooth footwall conditions created by the soft shale rock mass 34
Figure 4.4: Photos from different stopes showing the uneven hangingwall conditions in the west mine stopes 35
Figure 4.5: Uneven footwall conditions created by the hard and brittle quartzite rock mass 36

Figure 4.6: Top block of 116/65 raise (a) in shale footwall and 116/35 raise (b) showing the loss of ground with red hatching due to rockburst or increase in seismic activity ahead of the stopes 37
Figure 4.7: Plot of the average UCS values for each rock type specimen found in the three zones at Mponeng Mine 38
Figure 4.8: Plot of the average calculated Young's Modulus result for each rock specimen found in three footwall zones at Mponeng Mine 39
Figure 4.9: Plot of the average calculated Poisson's ratio result for each rock specimen found in three footwall zones at Mponeng Mine 40
Figure 4.10: Map3D numerical closure modelling results of the same area using the Shale properties (left) and quartzite properties (right) 41
Figure 4.11: Modelled ERR results using the shale and quartzite mechanical properties..... 42
Figure 4.12: Plan of 116/65 (Booysen's shale footwall) showing the geometry of the mined-out area and the nearby geological structures. 43
Figure 4.13: Plan of 116/35 (quartzite footwall) showing the geometry of the mined-out area and the nearby geological structures. 44
Figure 4.14: Number of seismic events with ML≥1.0 per raise-line for each year, with the total investigated rock mass damage. A=Quartzite Footwall, B=Shale Footwall..... 45
Figure 5.1: The σ_1 vs σ_3 plot based on the Hoek-Brown failure criterion for each rock mass encountered at Mponeng Mine 49
Figure 5.2: A plot of Young's modulus and Poisson's ratio from the lab tests 50

Figure 5.3: Total burst-type events recorded in the 116/65 raise-line vs in the 116/35 raise-line. A=Quartzite Footwall, B=Shale Footwall..... 51
Figure 5.4: Location of burst-type events to the active panels or the nearest panel in the raise-line of concern 52
Figure 5.5: Stress fractures around a deep stope mined in strong, brittle quartzite 55

LIST OF TABLES

Table 5.1: Estimated m_i values for each rock type and the calculated σ_1 value for each fixed σ_3 value 48

Table 5.2: Same magnitude event comparison between 116/65 and 116/35 53

Table 5.3: Different magnitude events but same distance to the face comparison between 116/65 and 116/35 53

APPENDIX LIST OF TABLES

Appendix Table 1:UCM results for the hangingwall and footwall core samples taken from the three footwall zones found at Mponeng Mine i

LIST OF EQUATIONS

Equation 2.1: Energy release rate calculation formula in mines 19

Equation 2.2: Hoek-Brown failure criteria equation 24

LIST OF ABBREVIATIONS AND SYMBOLS

CLR – Carbon Leader Reef

ERR – Energy Release Rate

GSI – Geological Strength Index

GPa – Giga Pascals

ISRM – International Society of Rock Mechanics

M_L – Local Magnitude

MPa – Mega Pascals

t/m^3 – tonnes per cubic meter

VCR – Ventersdorp Contact Reef

UCS – Uniaxial Compressive Strength

UCM – Uniaxial Compressive Strength with Modulus

σ – stress

ε - strain

υ – Poisson's ratio

E – Elastic/Young's modulus

1 INTRODUCTION

Mponeng Mine is in the West Wits mining district, approximately 80 km southwest of Johannesburg (**Figure 1.1**). In 2020, Harmony Gold acquired Mponeng Mine from AngloGold Ashanti. It is an ultra-deep mine that mines at depths greater than 3400 m below the surface, exploiting the Ventersdorp Contact Reef (VCR) via a twin-shaft system. Mining is currently concentrated in the B120 mine extension project, which is composed of two levels, 123 and 126. Additional levels will be added in the future.

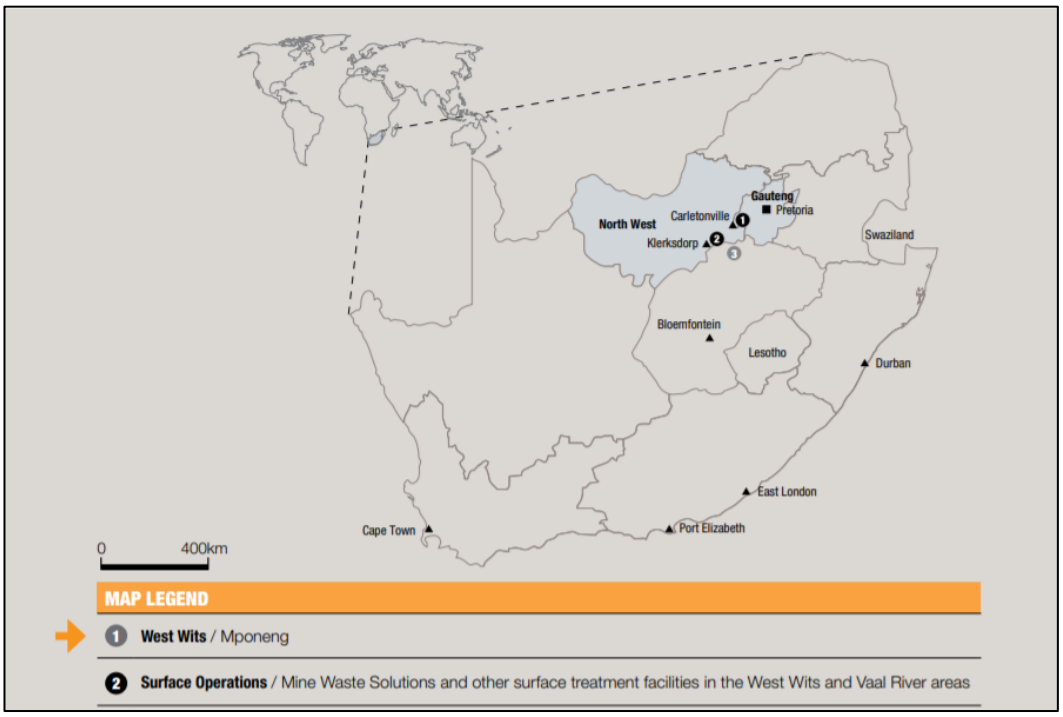


***Figure 1.1**: South African map showing the location of Mponeng Mine near Carletonville.*

As Roberts and Schweitzer (1999) mentioned, the VCR is one of the major gold-bearing orebodies found in South Africa. It separates the Witwatersrand Supergroup, which is predominantly composed of sedimentary lithologies at the bottom, from the Ventersdorp Supergroup, which is of volcanic lithology at the top.

The Witwatersrand Supergroup footwall is formed from undulating and highly variable sedimentary lithologies, which include the Booysens Shale, Jeppestown Shale, Conglomerates and Quartzite lithologies (Roberts and Schweitzer, 1999).

There are three footwall zones at Mponeng Mine where mining is currently concentrated. These are:

- Elsburg/Denny's quartzite footwall in the extreme Western part of the mine;
- Kimberley quartzite footwall in the middle of the mine, towards the Western part of the mine; and
- Booysens shale footwall in the Eastern part of the mine.

The UCS for all three footwall lithologies were tested. Though the Elsburg/Denny's quartzite and Kimberly quartzite have different physical characteristics, they are both quartzite lithologies and have been found to have a similar strength and failure behaviour. This study compared the shale footwall in the eastern part of the mine and the quartzite footwall in the western part, regardless of whether it is Kimberley or Denny's quartzite.

Seismicity is the biggest challenge in deep gold mines, resulting in loss of lives and production. In the past, seismicity was considered an act of God. This is, however, an unacceptable belief. Therefore, it is important to understand the factors that contribute to the generation of seismic events and how the mechanical properties of the rocks may contribute to the resultant rock bursts. This will ultimately help in making good mine design decisions and support strategies. Over the years, the assumption has been made that rock mass stability depends on the hangingwall rock mass, which is the same throughout the mine. The modelling inputs have never considered the difference in footwall; therefore, the mine layout and support strategy have been kept the same in all footwall zones.

1.1 Research Background and Context

Scheepers et al. (2012) studied the effects of seismicity at Mponeng Mine, and they correlated seismicity to the rate and volume of mining. Their studies did not consider the mechanical rock properties and how they influence the seismic distribution. The mining layouts were reviewed, and dip pillars were introduced to limit spans and effective closure; however, the study was not based on each geotechnical zone. There are three footwall zones at Mponeng Mine where mining is concentrated. The properties of the intact rock types in these footwall zones

differ, and the failure behaviour during a seismic event also differs. These footwall zones are:

- the Elsburg/Denny's quartzite footwall in the extreme western part of the mine;
- the Kimberley quartzite in the middle and towards the western part of the mine; and
- the Booysen's shale footwall in the eastern part of the mine.

Though there are three footwall zones, the geotechnical zones are defined as the Booysens shale footwall and the quartzite footwall. However, the mining and support strategy between the two geotechnical zones is the same.

In 2017, three seismic-related incidents resulted in multiple losses of life. Two incidents were in the west mine (quartzite footwall) and one in the east mine (shale footwall). The magnitudes of the two seismic events on the west mine were less than the magnitude of the seismic event recorded on the east mine; however, the size of the resultant damage from the two events on the west mine was significantly more than the size of the resultant damage on the east mine. This raised a concern and a need to investigate and research the factors that influenced the rock mass response to seismicity in each geotechnical zone. The historic seismic activity and damage between the two geotechnical zones were investigated to determine how they differ and the factors that influenced the response. The mechanical properties of the intact rocks and physical properties of the rock masses in each zone were determined. The physical appearance of each rock surface and the petrology of each rock type were studied. The mechanical properties included the uniaxial and tensile strength, Young's modulus and Poisson's ratio. The study correlated the observed damage with the intact rock properties.

1.2 Problem Statement

There is a clear contrast in the severity of rock burst damage between the two footwall zones. This research addresses the following:

i. How are the mechanical properties of each rock type influencing the behaviour of the rock mass during a rockburst?

ii. Mine design and support strategies in each of the two geotechnical zones.

1.3 Justification for Research

Mining at Mponeng is conducted under high-stress and seismic conditions (Scheepers et al., 2012). This study aimed to improve and/or optimise the mining layouts to manage seismicity and optimise the support strategies to minimise the rockburst impact.

1.4 Research Objectives

Historical data have shown that significant damage has been observed in the western part of the mine, where the footwall is composed of quartzite lithologies, compared to the comparatively smaller damage observed in the eastern part of the mine, where the footwall is composed of shale lithologies. The factors that influence the difference in the rock mass failure during a seismic event in these geotechnical zones have never been studied. The objective of this research was to determine why there is such a large difference in the rock mass response during dynamic loading caused by the seismic events. This will be done by:

- Analysing the characteristics of the seismic activity and the events near the active stopes;
- Analyse the deformation and failure mechanisms triggered by the seismic events; and
- Use numerical modelling to simulate and validate rock mass behaviour in each footwall zone.

1.5 Research Methods

This study included both qualitative and quantitative research methods. The qualitative research methods included underground observations and the analysis of the investigated falls of ground (FOG) in each geotechnical zone. The quantitative research methods included the laboratory testing of each rock type from the different footwall zones to determine the compressive and tensile strength. The determined mechanical rock properties were then used in numerical

modelling to simulate and validate the rock mass behaviour in each geotechnical zone. The research will be done by:

- analysing the magnitude of the rock mass damage caused by seismic events in each of the two zones, where the magnitude range is similar, located at similar distances from the affected panels and having the same source mechanism;
- determining the intact rock properties of each rock type found within the two geotechnical areas using laboratory tests; and
- investigating the physical rock conditions in different panels within each footwall zone to determine if there are other physical factors which contribute to the failure behaviour of the rock mass during a seismic event.

Extensive investigations of the falls of ground were conducted at Mponeng Mine and well documented for each geotechnical zone. These reports were not analysed to differentiate between the two zones. Though it has been known that these areas behave differently, there was no research to understand why they behave the way they do. From simple analysis, one would expect the shales to have more damage as they are the weaker rock mass.

1.6 Source of Data

Several sources of data were used, which included the following:

- the intact rock strength was determined in the Wits laboratory using the standardised methods of testing according to the International Society of Rock Mechanics (ISRM) (Ulusay and Hudson, 2007);
- the ground conditions in each geotechnical zone were gathered from underground visits at selected workplaces;
- the data for the historic falls of ground due to seismicity were gathered from the fall of ground investigation reports in the Mponeng mine database; and
- seismic information of the events in the two chosen workplaces was provided by the Institute of Mine Seismology.

1.7 Research Validation

The need for a higher support resistance and smaller stopes in the areas of quartzite footwall was validated by the comparatively more brittle failures in the quartzite laboratory tests and visual observations underground.

1.8 Structure of the Research Report

This report consists of six chapters. Chapter 1 is the introduction and covers the background of the research topic, the problem statement, the justification for the research, and the research objectives. The research methodologies followed by this study and the sources of the information are introduced. The research validation criteria, as well as the contribution to knowledge, are discussed.

Chapter 2 reviews the available literature that explores all the theories and key concepts of the study. The chapter will explore the key debates and controversies on the subject. The stratigraphy of the mine was reviewed in detail in this chapter, and the characteristics of each rock mass were explored to justify why it behaves the way it does during dynamic loading.

Chapter 3 will explain the design process of the research and how the data used were collected. A data validation process will be explained and compared to the

known concepts and theories. The approach that will be used to analyse the data will be detailed in this chapter before the data for the study is presented in the next chapter.

Chapter 4 will present all the collected data for the study and explain the importance of each data set in the study.

Chapter 5 will then analyse the data and all the research findings.

Chapter 6 concludes the results analysis and gives recommendations on the immediate changes that can be implemented and additional studies that can be done to improve the mine design.

2 LITERATURE REVIEW

2.1 Introduction

The rock mass response in each geotechnical zone should be part of the rock engineering design elements. The understanding of each zone in terms of how the rock mass behaves and how it contributes to the seismic response of each zone should be a consideration during the rock engineering design inputs. This chapter will investigate the key concepts, theories, and studies that have been conducted in similar environments. The key debates and controversies will be explored from the available literature.

2.2 Key Concepts, Theories and Studies

2.2.1 The Ventersdorp Contact Reef

The Ventersdorp Contact Reef (VCR) was first discovered in 1886 and first exploited in 1888 (de Kock, 1940; Reimold and Viljoen, 1994; Richardson and van Helten, 1984). The VCR became one of the major gold-bearing conglomerate reefs in the Witwatersrand Basin. The Witwatersrand Basin was described in Ryder and Jager (2002) as an inland sea that eroded auriferous containing bodies of the Basement granites and greenstone belts. The gold and other heavy minerals were then sorted and concentrated by the fluvial systems together with gravels and pebbles, forming the ‘gold reefs’ (Ryder and Jager, 2002). There are a lot of different types of reefs striking and dipping in different directions. The VCR occurs in the Carletonville area, but is not exploited at all the mines in the area as indicated by Ryder and Jager (2002). Chunnett (1994) (as cited in Ryder and Jager, 2002) mentioned how the production increased from the VCR over the years, making it the single largest contributor of total gold in the mining industry.

According to Ryder and Jager (2002), most of the stoping was taking place at depths that range between 2000 m – 3000 m below the surface. The current stoping of the VCR at Mponeng Mine is now beyond 3600 m below the surface, making it the deepest mine in the world.

2.2.2 Lithology of the VCR

There are two economic reefs found at the Mponeng mining lease, i.e. the VCR and Carbon Leader Reef (CLR). VCR is currently the only reef being mined due to the high capital costs associated with deepening the shaft to access the CLR, which is situated about 900 m below the VCR. VCR is one of the major gold-bearing orebodies in South Africa. VCR separates the Witwatersrand Supergroup, which is predominantly composed of sedimentary lithologies, from the Ventersdorp Supergroup, which is of volcanic lithology (**Figure 2.1** and **Figure 2.2**) (Roberts and Schweitzer, 1999).

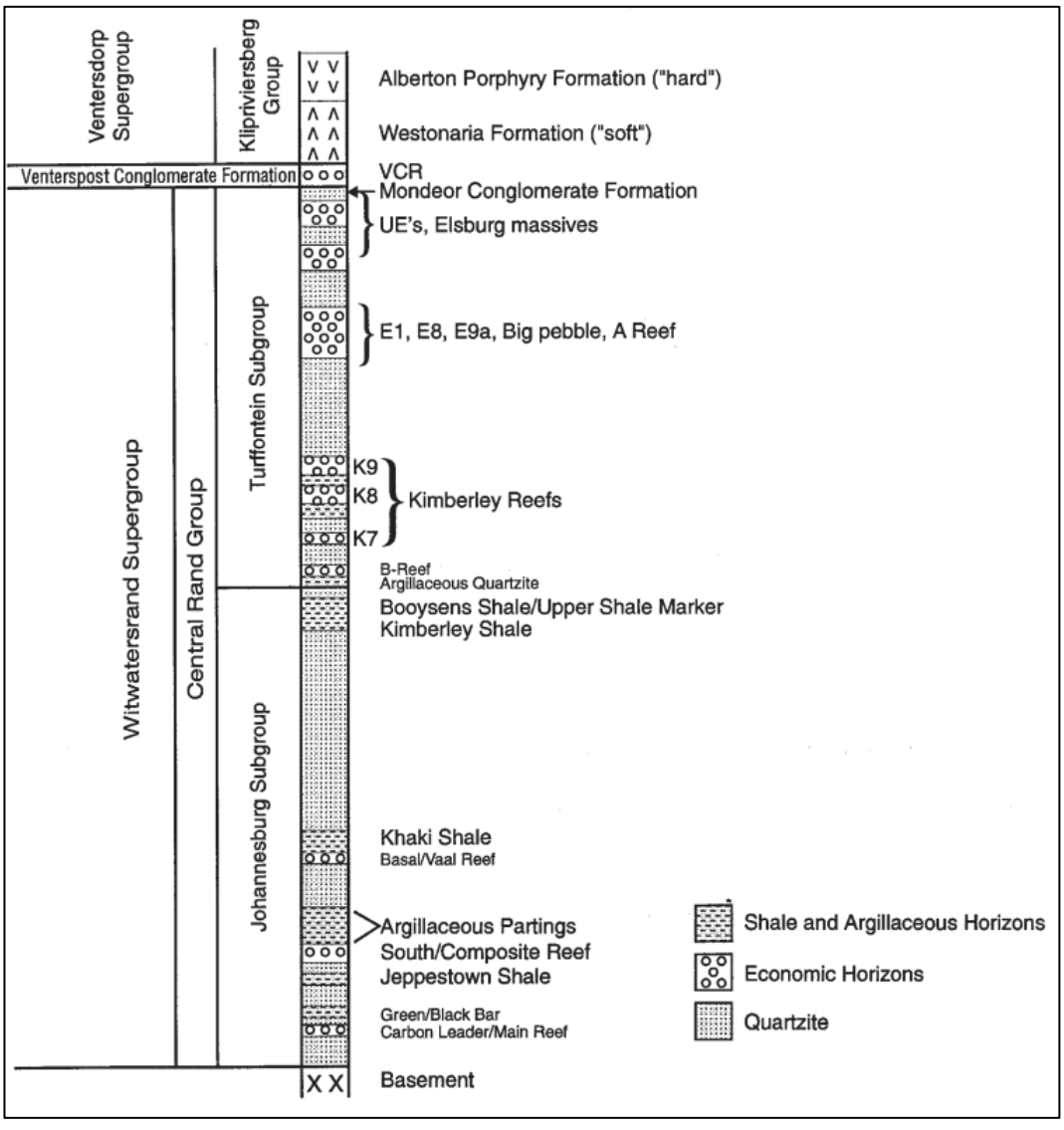


Figure 2.1: *Stratigraphy of the Witwatersrand Supergroup. (Roberts and Schweitzer, 1999)*

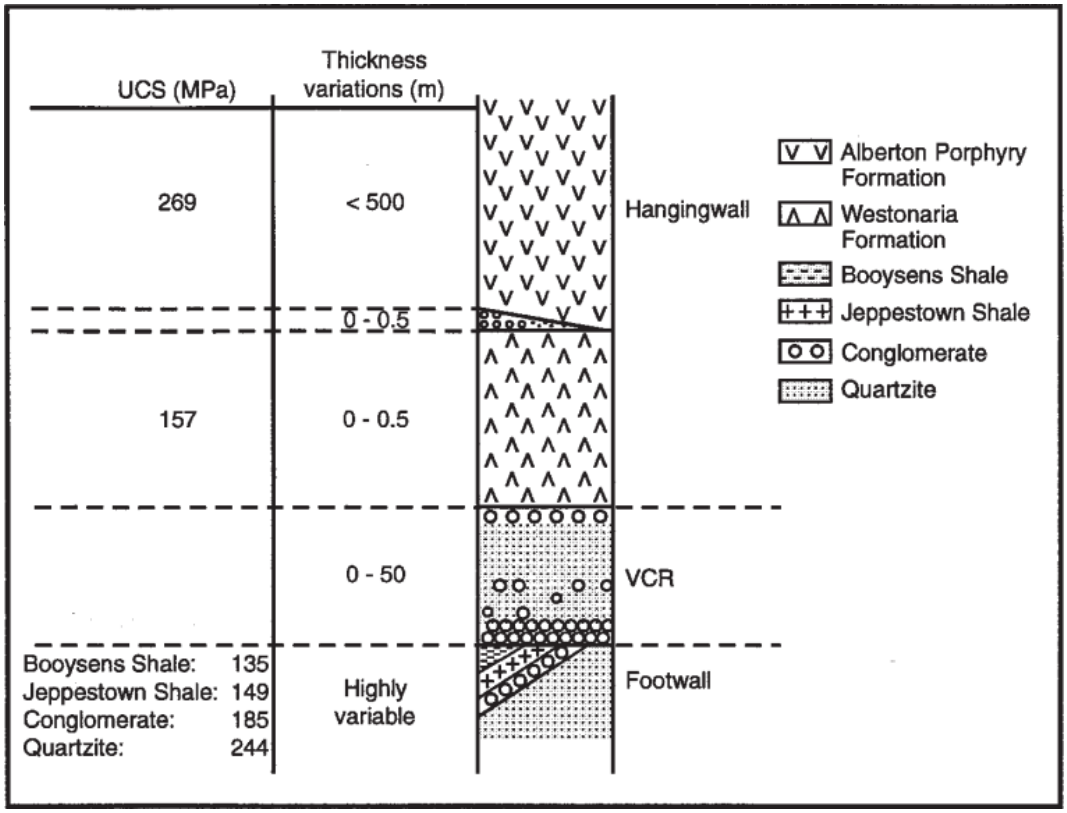


Figure 2.2: *Idealised VCR stratigraphy showing the UCS of the over- and underlying rocks (Roberts and Schweitzer, 1999)*

VCR is considered a basal unit of the Ventersdorp Supergroup and is unique with a lava hangingwall and different types of footwall lithologies (Ryder and Jager, 2002). Two types of hangingwall lava are found above the VCR at varying thicknesses, i.e. the Westonaria formation, which is the soft lava and the Alberton Porphyry formation, which is the hard lava (Duraprai, 2015; Roberts and Schweitzer, 1999). The Ventersdorp Supergroup from borehole data in various areas has been found to have a thickness that ranges from 1800 m to over 3000 m (Winter, 1976).

The hangingwall at Mponeng Mine is composed of hard Alberton Porphyry formation lava (**Figure 2.3**) (Roberts and Schweitzer, 1999). The hangingwall lava is basaltic, which means that it has a high iron and magnesium content (Bester, 2019).

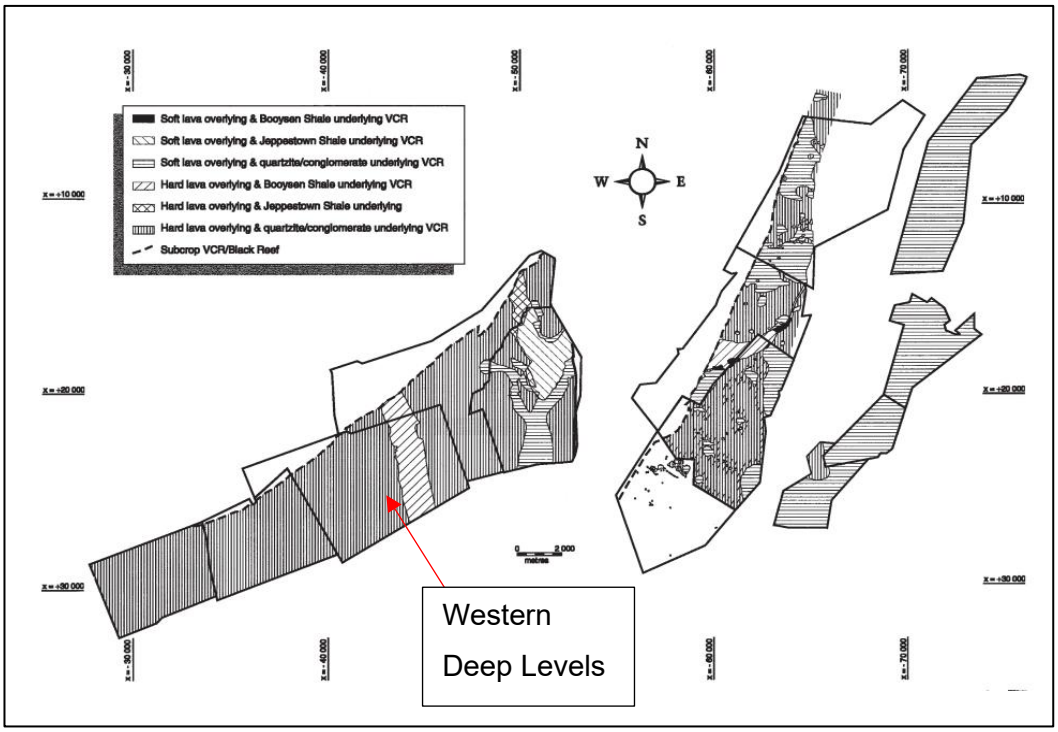


Figure 2.3: *The geotechnical zones of the VCR in the Witwatersrand Basin mines indicate the position of Western Deep Levels mines. Modified from: (Roberts and Schweitzer, 1999)*

The hangingwall lava is, however, not uniform across the Mponeng Mine. The physical conditions vary from area to area, though the mineral composition is the same. As lava was formed from molten magma, the cooling process was not constant, resulting in the formation of different mineralization and weakness zones. Though there is a slight difference, it is all classified as hard lava due to the high UCS values.

Grove (2006) identified two lithologies, which are:

i. Aphanitic lava (**Figure 2.4**) – this is the most competent lava, which is a result of fast cooling. Due to fast cooling, the texture becomes smoother and consistent as there is no time for mineral crystallization; however, gas bubbles can be trapped in the process, which might lead to weaknesses in the rockmass.

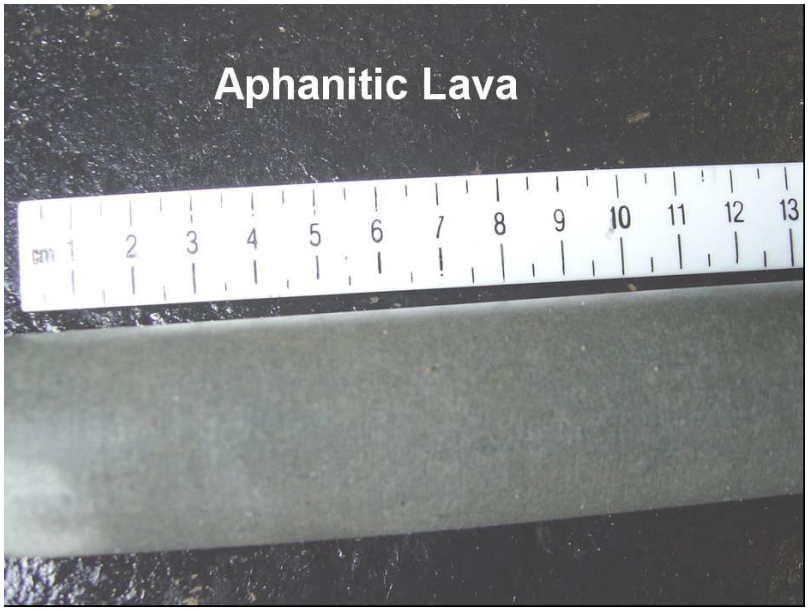


Figure 2.4: *Photo of an aphanitic lava rock sample from a drill core*

ii. Porphyritic lava (**Figure 2.5**) – this lava cooled more slowly, therefore allowing for the formation of the feldspar phenocrysts.

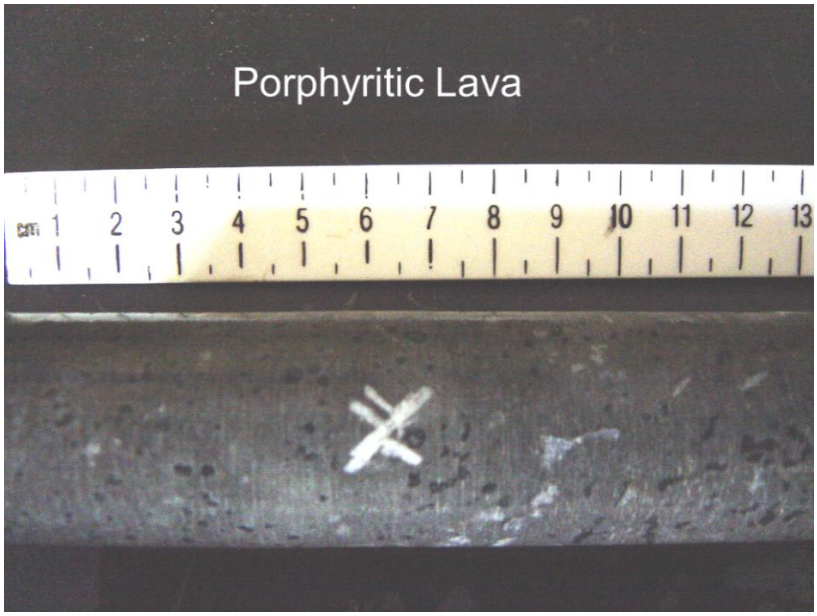


Figure 2.5: *Photo of a porphyritic lava rock sample from a drill core*

There are three main footwall lithologies at Mponeng Mine (**Figure 2.6**). These footwall lithologies are:

- Elsburg/Denny's quartzite footwall in the extreme Western part of the mine;
- Kimberley quartzite footwall in the middle of the mine towards the Western part of the mine; and
- Booysens shale footwall in the Eastern part of the mine.

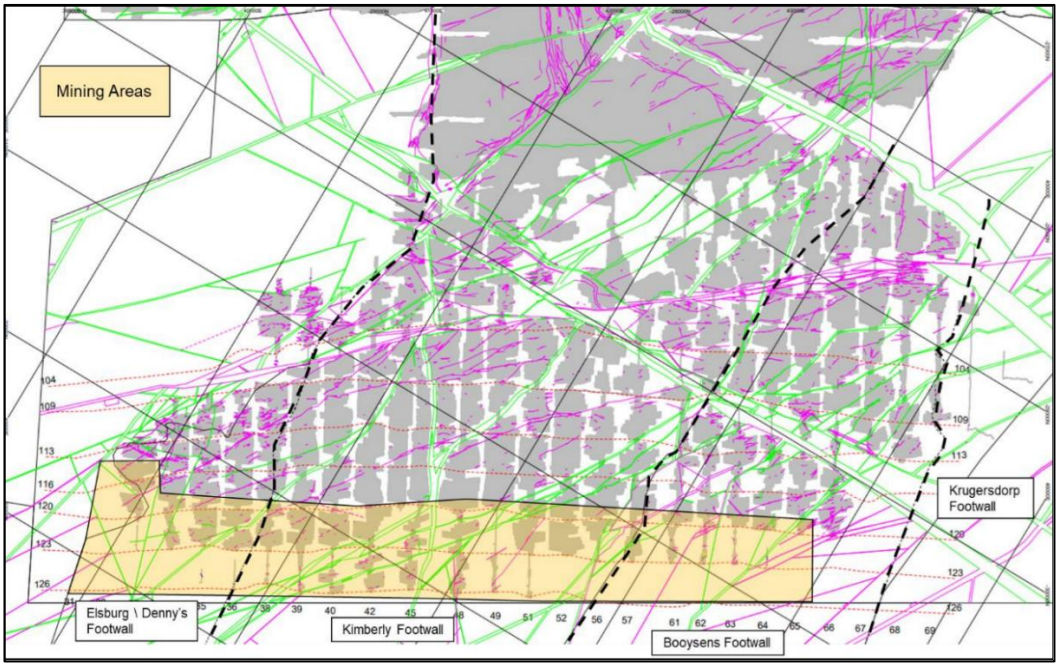


Figure 2.6: *Plan of Mponeng mine showing the location of different footwall zones compared to the current and planned mining area as per the LOM business plan*

The quartzite lithologies are the most competent due to their high compressive strength. However, as observed during uniaxial compressive tests in the laboratory, they fail in a brittle manner. Therefore, from the underground observations in the access tunnels, the Kimberley quartzite tends to result in excessive sidewall scaling. The Booysens shales are a major concern to the stability of the off-reef development, especially the excavations striking parallel to the strata. The underground observations have shown less sidewall scaling; however, it bulges into the excavation under plastic horizontal movement. The laminated hangingwall beam has resulted in massive collapses due to the lack of or insufficient clamping of the laminations, which fail in tension. This, therefore, results in poor ground conditions in the off-reef access ways. More focus was put

on the off-reef development mining through Booysen's shales. The influence of these two lithologies was never considered during the design of the stope layouts and support; however, they influence the stope stability.

2.2.3 Mining sequence and support strategy

The shallower depth sections of Mponeng Mine, north of the shaft pillar, were mined using the longwall mining method. Due to the increase in stress as the depth of mining increased, the mining method was changed to a sequential grid. This mining method has the advantage of having regularly spaced regional pillars (dip pillars, strike pillars and bracket pillars) which assist in managing the seismic hazard (Scheepers et al. 2012). The challenge with this mining method is that it reduces the extraction ratio. Scheepers et al. (2012) indicated that the extraction ratio was about 64%. The regional stability pillars (30m wide for dip and strike pillars, and 20m wide for bracket pillars on each side of the geological structure) combined with the cyclone classified tailings backfill placed in all the stopes not more than 5m from the face are the primary strategies to manage the seismic hazard (Sheepers et al., 2012; McGill et al., 2023).

In the Mandatory COP (McGill et al. 2023), the following factors contribute to the rate and intensity of seismic activity:

- Frequency of occurrence of geological features, especially faults and dykes.
- Angle of approach to geological features, especially faults and dykes.
- Mining span.
- Extraction sequence and configuration.
- Rate of mining and mining volume.
- Regional support system characteristics.
- Effective length of panel (small lead lags distances are perceived to result in an effective longer panel length) or abutment.

In 2019, the ideal stope profile was assessed to manage the seismicity ahead of the stopes. The study highlighted the importance of lead-lag and panel lengths in a profile to manage the stress distribution ahead of the stope profile (Rakumakoe,

2019). The standard at Mponeng Mine was revised to limit the panel length to 30m measured from gully to gully with a lead-lag of 7-13m. The limited panel length and lead-lag has managed to reduce the seismic hazard (Rakumakoe, 2019).

Designing support in a rockburst-prone environment should consider the dynamic resistance capabilities of the chosen support units (Kaiser and Cai, 2012). Malan and Napier (n.d.) wrote a paper that focused on the face support with energy absorption capabilities to resist rockbursts, combined with areal coverage support. Props, packs, tendons and backfill are used in combination to stabilize the rockmass and reduce the risk of fall of ground and rockbursts (Daehnke et al., 2001). Backfill is said to have the capability of reducing the energy release rate and associated seismicity; however, it is complex and expensive to set up, and therefore, is not used in all mines (Malan and Napier, n.d.). The elongates and timber packs are mostly used close to the stope face; however, they lose the capability to withstand dynamic loading as the distance from the face increases due to elastic convergence. The design of the support in dynamic conditions is complex, and there are no models to explain how the support systems work (Kaiser and Cai, 2012). The tributary area concept is used in the design of the stope support system where the weight of the hanging wall is determined by the possible fall-out height and divided between the fixed number of support elements (Daehnke et al., 2001). Figure 2.7 shows the flowchart indicating the principal design steps of support design methodology (Daehnke et al., 2001). Short bolt length (typically 0.9m) has been integrated in the support system, but mostly to support the small rock falls between the elongate and pack support units, not for dynamic loading (Malan and Napier, n.d.).

Though Malan and Napier (n.d.) indicated that areal coverage support is difficult to implement in the narrow reef stopes, Mponeng Mine has successfully implemented areal coverage support in terms of permanent steel nets secured to the hanging wall with 0.9m tendons, 0.2m from the face. The tendons are installed in between the yielding elongates. The back areas are supported with backfill from cyclone-classified tailings.

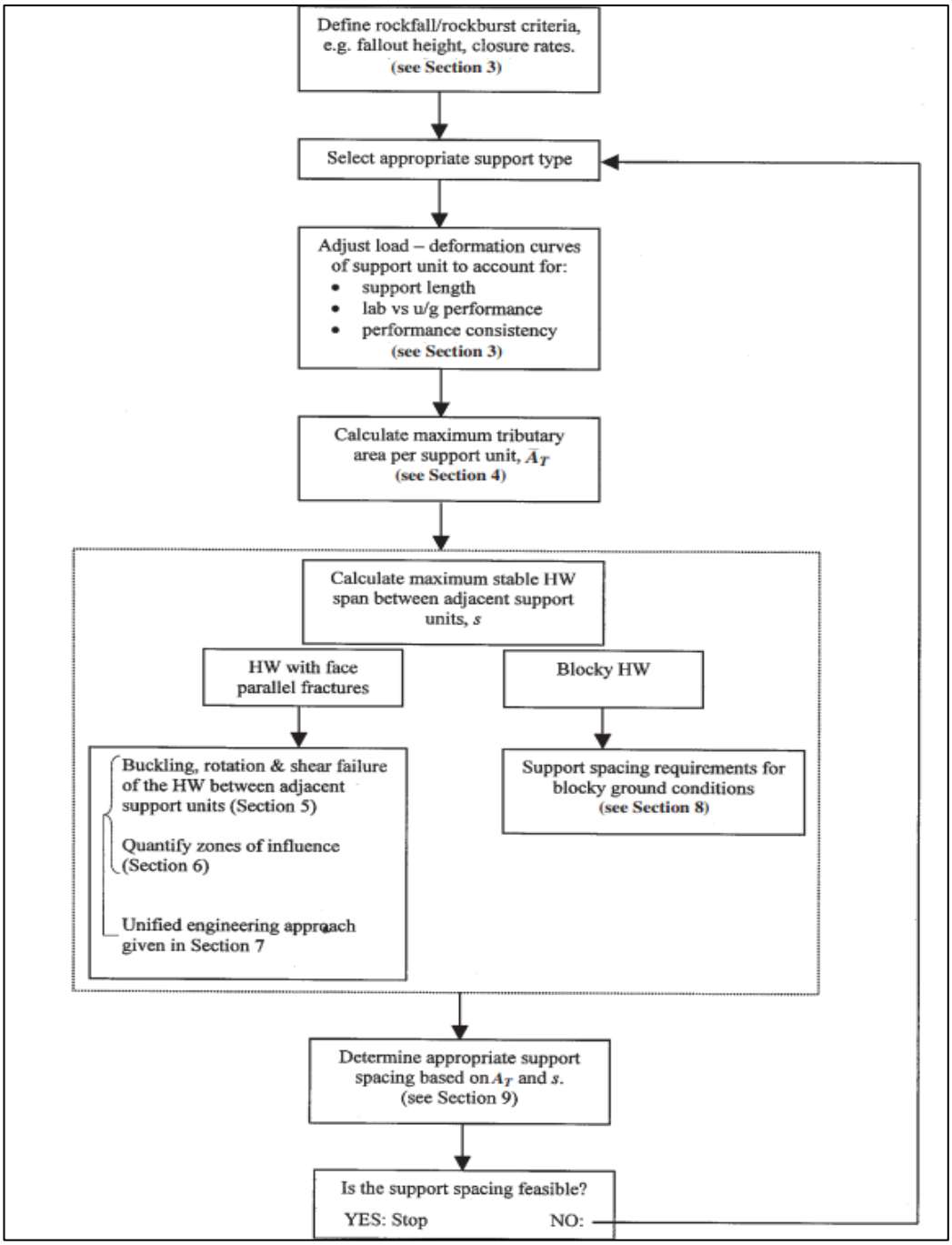


Figure 2.7: *Flowchart indicating principal steps of support design methodology (Daehnke et al., 2001)*

2.2.4 Seismicity and Rockburst

VCR mining in the Witwatersrand gold mines is getting deeper and becoming more challenging. Ryder and Jager (2002) described a seismic event as “a sudden inelastic deformation within a given volume of rock, whereby a source radiates

detectable seismic waves" (Ryder and Jager, 2002). Seismicity has been a concern to the mining communities since the early 1900s after the discovery of gold and commencement of mining in Johannesburg (Durrheim, 2010; Durrheim et al., 2006). Research has been done to understand the factors that influence seismicity by Durrheim et al. (1998), and an investigation into methods to try and predict seismicity by Hagan (1981). Mponeng mine, as the deepest mine in the world, has very high vertical virgin stress and, therefore, high seismicity (Scheepers et al., 2012).

Seismicity is a huge problem in deep deep-level gold mines of South Africa. Seismic events that cause damage are defined as rockbursts (Jager and Ryder, 1999). The Rockburst Commission Working Group of the International Society of Rock Mechanics (ISRM) defined seismic events and rockbursts in Jager and Ryder (1999). Rockbursts are unwanted events in the mines as they lead to injuries and/or loss of life, equipment and production. Historically, seismicity has been the largest cause of mine fatalities and serious injury accidents. With the change in mining and support strategies and the reduction in production over the years, the seismic activity rate has significantly decreased at Mponeng Mine, but it remains one of the major contributors to mine accidents. The focus of this project is on potentially damaging seismic events, which will be from 1.0 M_L and above. Magnitude alone does not completely describe the potential for damage, but it has been found that there is a direct correlation between an increase in event magnitude and an increase in the potential for rock damage (Scheepers et al., 2012). Scheepers et al. (2012) also mentioned that the distance of the seismic event to the excavation face plays a very important role in the extent of damage of the excavation. This means that the closer the event is to the excavation, the higher the potential of causing damage. Seismic event location to the nearest panel face was considered in the comparison between seismic events on the east and west sections of the mine.

2.2.5 Seismic event sources

Croll and Walker (1973); Thompson and Hunt (1973) (as cited by Brady and Brown, 2004) determined that the stability of the mine is based on the principles of stability of equilibrium. This requires that "any small change in the equilibrium state of loading of a structure can provoke a sudden release of energy or large change in the geometry of the structure" (Brady and Brown, 2004). Brady and Brown (2004)

mentioned that the small changes might be caused by blasting vibrations, a change in mining volume, local failure, increased extraction ratio, and an increase in depth of mining.

There are two main seismic source categories described at the Mponeng mine as defined in the Code of Practice:

- Events associated with slip on geological features, generally larger magnitude events which occur mainly on major geological structures such as faults and dykes; they are governed by the overloading of the structure and friction properties of the discontinuity; and
- Events associated with abutment and mining faces are smaller magnitude events, but can be large events on long abutments; they are the common type of events resulting from fracture formation in the solid ahead of the faces of abutments.

McGarr et al., 1975; Gibowicz, 1984; Stiller et al., 1983; Wong, 1985 (as cited by Wong, 1992) classified the seismic events into two categories according to their location with the mine workings:

- Events that occur very close to the active working places because of stress concentration and failure near the excavation; and
- Far-field events or sometimes close to the mining places, but appear to be caused by the interaction of mining-induced stresses and the tectonic stress field.

Wong (1992) also mentioned that seismicity can be classified by the mode of failure. The two modes of failure are fracturing of intact rock ahead of the stopes and slipping along the pre-existing zones of weakness. Within the vicinity of the mine abutments, the stress concentration is highest, which results in the seismic events associated with the formation of new fractures. Seismic events associated with geological structures can be close or far from the working places (Wong, 1992).

Durrheim et al. (1998) investigated the factors that influence the severity of rockburst damage. They mention mitigating factors like stabilizing pillars, mining

layouts and sequencing, in situ stress, faults, face shape, etc. These factors influence the severity of rockburst damage. Production volume and type of rock also contribute to the number and magnitude of seismic events recorded in a mining area (Scheepers et al., 2012). Durrheim et al. (1998) recorded that the lava above the VCR has higher uniaxial compressive strength and Young's Modulus than the reef. The lava, therefore, stores more strain energy than the reef, resulting in a relatively higher incidence of face bursts.

2.2.6 Energy Release Rate

Deep-level mining is associated with high stress. The stress is concentrated ahead of the mining faces in the solid rock. The high stress leads to fracture formation and extension. During the process of forming a fracture on the solid rock or a fracture extending, strain energy is released (Wang, 1996). This process is referred to as the Energy Release Rate (ERR). This leads to the generation of burst-type seismic events ahead of the mining faces. Energy Release Rate (ERR) is defined by the stress just ahead of the face and the deformation that occurs when that rock is removed (Ryder & Jager, 2002). This concept is used as a design tool for stope configurations to minimise rockburst potential in deep-level mining (Jager & Ryder, 1999). A higher ERR suggests a higher risk of a large seismic event.

Milev and Spottiswoode (2002) used the energy release rate to obtain the changes in the volume of convergence. The energy release rate was calculated using the following formula:

$$ERR = \frac{\sigma D}{2} \qquad \textit{Equation 2.1}$$

Where σ is the stress before an element is mined and D is the convergence between the hangingwall and footwall after the element is mined. Considering this calculation, it indicates that the shale footwall will have a higher ERR as there is higher convergence than in the quartzite footwall. Salamon (1984) defined ERR as a representation of energy released (or stored) per area mined. The shale footwall

was, therefore, expected to have a higher ERR, generating larger seismic events. However, the energy is released through fracture formation.

2.2.7 Intact rock strength

The intact rock is referred to as the rock material with no visible discontinuities, whereas the rock mass is the combination of the intact rocks, fractures and weathering profile (Singh and Goel, 2011). Ozturk et al. (2014) mentioned that the intact rock material and discontinuities affect the strength of the rock mass, whereas the mineral composition of the rock affects the strength of the intact rock. Hoek (1994) suggested that to understand the behaviour of jointed rock masses, the intact rock material should be studied. The intact rock pieces will respond by translating, rotating or crushing to the stress to which the rock mass is subjected, depending on the nature, amount and orientation of the discontinuities. It is, therefore, important for rock engineers to know the strength of the intact rock to help with the prediction of the strength of the rock mass.

The hangingwall lava above the VCR at Mponeng Mine is the hard Alberton Porphyry formation lava. Roberts and Schweitzer (1999) mentioned that the UCS of the hard lava hangingwall is in the range of 270 MPa. Jager and Ryder (1999) summarised the properties of different rock types found in the gold and platinum mines. These authors suggest that the uniaxial compressive strength of the lava varies between 200 MPa and 500 MPa, while quartzite and shale vary between 200 MPa and 300 MPa and 80 MPa and 200 MPa, respectively. Drescher and Handley (2003); Kaiser and Cai (2013), on the other hand, stated the UCS values of Witwatersrand quartzite and the Ventersdorp Lava to range between 100 MPa and 250MPa and 200 MPa and 300 MPa, respectively. These ranges in UCS values are very wide, and therefore, it is important to conduct site-specific tests to get a mean value of UCS.

The off-reef development through the Booysens shales has been a strata control concern where multiple incidents of hangingwall failure have been recorded. The geology department at Mponeng Mine in 2015 delineated different zones of the Booysens shale intersection in the off-reef development after several failure incidents on the 123 and 126 Levels. The shale package was separated into four zones depending on the amount of shale content as per the Mponeng Mine's

Mandatory Code of Practice to Combat Rockfall and Rockburst Accidents in Tabular Metalliferous Mines (McGill et al., 2023):

- Zone A has 90% of shale content and is, therefore, the weakest;
- Zone B is 50% shale and 50% siltstone;
- Zone C is 10% shale and 90% siltstone; and
- Zone D is a massive siltstone, which is the most competent portion of the Booysens shale package.

Zone A shales are of major concern as they are highly laminated. The lamination results in them being the least competent as they are more prone to tensile failure along the hangingwall of the off-reef development excavations, especially Haulages and Return Airways (RAW) striking parallel to the strata. Shale is a soft/weak rock mass that exhibits time-dependent behaviour, resulting in tunnel instability problems (Bonini et al., 2007). The shale material, unlike the hard and brittle quartzite material, tends to exhibit a creep-type of failure. Creep is defined as “irreversible ductile deformation in time under constant stress”(Ghosh Roy and Rao, 2015). Creep is rare in the hard-brittle rocks, as the rate of deformation is extremely slow (Drescher and Handley, 2003; Ghosh Roy and Rao, 2015). Creep explains why there is a high rate of footwall heave in the stopes with shale footwall and why there is a ductile failure of the sidewall in the off-reef excavations mined through shale. Softer, less brittle rock types inherently have significant creep even in shallow, low-stress mining environments (Drescher and Handley, 2003).

The uniaxial compressive strength (UCS) and Brazilian tensile strength (BTS) of rocks are commonly used by rock engineers in the design of surface and underground structures. This is, however, a costly and time-consuming process. Kahraman et al. (2012) suggested the use of indirect tests, which are a better alternative since they require little or no sample preparation and the equipment for testing is very simple. The simplicity of the indirect tests allows for the tests to be conducted even in the field. The index test methods include the point load index (I_s) and the Schmidt rebound number (R) (Ozturk et al., 2014). As mentioned by Kahraman et al. (2012) and Bieniawski (1974), Rock Engineers commonly require only two rock-material properties for the design of underground excavations, i.e. UCS and BTS. Armaghani et al. (2014) emphasised the importance of determining

Young's Modulus (E) for the design of geotechnical engineering structures. The methodology for testing the UCS of intact rock has been standardised by the International Society of Rock Mechanics (ISRM, 1981) and the American Society for Testing and Materials (ASTM, 1984) (as cited in Ozturk et al., 2014).

The source of the laboratory samples is usually from diamond drilling, where a sample in the diameter range of 50 mm is used. The sample diameter needs to be greater than ten times the largest grain to ensure that grain size does not influence the strength result (Hoek and Martin, 2014). The laboratory tests for the quartzite and lava are easy, as the grain sizes are small. Shale samples may be difficult to provide due to lamination. Singh et al. (2001) and Monjezi et al. (2012) (as cited in Armaghani et al., 2015) expressed that it is difficult to prepare core samples of highly fractured, laminated, or foliated rocks.

The other three rock masses in this study are made of hard-brittle rock materials, which have less creep. However, significant closure is expected in the ultra-deep hard rock mines. The closure has time-dependent properties which are influenced by at least four mechanisms: "compression creep of the intact rock, rock material dilation arising from stress damage, shear creep on discontinuities, and discontinuity dilation with growing shear displacements"(Drescher and Handley, 2003). Scheepers et al. (2012) investigated the influence of closure on the rate of seismic response. The rate of closure is higher in the shale footwall than in the quartzite footwall, mostly due to the dilation of the softer shale footwall. Critescu and Hunsche (1998), as cited in Nyungu and Stacey (2014), argued that all types of hard rocks are prone to showing creep characteristics over a long enough time.

Zhang, Ranjith and Perera (2016) described brittle rocks as rocks that are subjected to sudden failure with the formation of tensile/shear fractures, which suddenly drop in strength with small inelastic strain. They also described the contrast where the ductile rocks undergo large inelastic deformation before failure. The laboratory tests show that the lava and quartzite rock samples have a sudden failure with multiple tensile/shear fractures developing. The lower Poisson's figure is a sign of small inelastic strain. On the other hand, the shale rocks have a higher Poisson's ratio, indicating a larger inelastic deformation before failure. Brittle and ductile are both post-failure behaviours; therefore, brittle rocks form more fractures

than ductile rocks. The hard quartzite and lava will consequently have more fractures than shale. The brittle rocks have a higher Young's modulus and a lower Poisson's ratio than the ductile rocks, which have a higher Poisson's ratio and a lower Young's modulus (**Figure 2.8**).

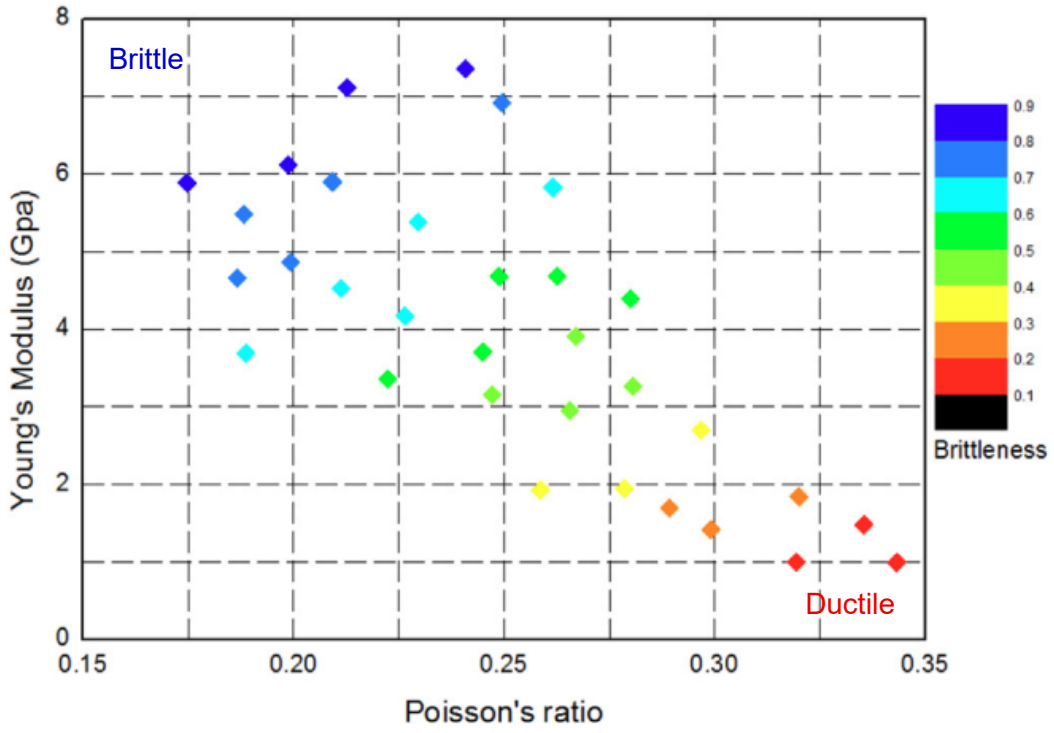


Figure 2.8: *Relationship of brittleness to Young's modulus and Poisson's ratio (Zhang et al., 2016)*

2.2.8 Rock mass classification

A rock mass, as mentioned earlier, is composed of intact rocks, fractures and weathering profiles (Singh and Goel, 2011). It is not possible to test the strength of a rock mass in the laboratory due to its large scale and having many variables that influence the rock mass strength. Rock mass classification systems are therefore used to determine a common behaviour of the rock mass surrounding the mining excavations. The rock mass description is determined using one of several classification schemes. The systems assign numerical values to the rock mass properties that are considered to influence its behaviour. These values are then combined to give a single overall classification rating for the rock mass (Brady and Brown, 2004).

Palmstrom and Broch (2006) explained that a rock mass classification uses observable and measurable variables from the field, which are then expressed as numbers. These numbers are combined into a single value that defines the rock mass. The final number can be compared to a table giving the quality description of the rock mass.

2.2.9 Rock mass strength

The rock mass strength is estimated using a rock mass strength criterion. There are several rock mass failure criteria available. The most used criteria are the Hoek-Brown failure criterion and the Mohr-Coulomb failure criterion.

The Hoek-Brown failure criterion assumes an isotropic rock and rock mass behaviour; therefore, it should only be used where the rock mass has multiple discontinuities which are closely spaced so that a pseudo continuum behaviour can be assumed (Hoek and Brown, 1997). The Hoek-Brown failure criterion was introduced in 1980 (Hoek and Brown, 1980a, 1980b) and then revised over the years, with the latest revision in 2018 (Hoek and Brown, 2019). The generalised Hoek-Brown failure criterion by Hoek (1994) and Hoek et al. (1995) (as cited in Hoek and Brown, 2019) is described by the following equation:

$$\sigma_1 = \sigma_3 + \sigma_{ci}(m_b \frac{\sigma_3}{\sigma_{ci}} + s)^a \qquad \textit{Equation 2.2}$$

Where m_b, s and a are the rock mass material constants calculated using the geological strength index (GSI), disturbance factor due to blasting and relaxation (D) and material constant (m_i) as stated in Hoek and Brown (2019).

The Mohr-Coulomb failure criterion is described as “a set of linear equations in principal stress space describing the conditions under which an isotropic material will fail. The intermediate principal stress is not considered (Labuz and Zang, 2012). Triaxial tests should be conducted at different confinement (σ_3) stresses to plot the Mohr-Coulomb failure envelope. The sigma 1 and sigma 3 test results are plotted on the same horizontal axis and joined with semi-circles using the difference between σ_1 and σ_3 as the diameter of the half circle. The failure envelope is a linear or non-linear tangent to all the circles.

2.2.10 Influence of rock strength on ground conditions

According to Jager and Ryder (1999), high stress around a stope with a similarly strong and brittle hangingwall and footwall results in the propagation of stress fractures (Jager and Ryder, 1999; Ryder and Jager, 2002). These fractures (**Figure 2.9**) can form unstable wedges, which result in rock mass failure between the support units during a seismic event. A stronger rock mass accumulates more strain energy, which can generate burst-type seismic events through fracture formation. The initiation and propagation of the fractures are therefore associated with ERR. This suggests that the stiffer system of quartzite footwall will have a higher energy release rate than the softer system of shale footwall.

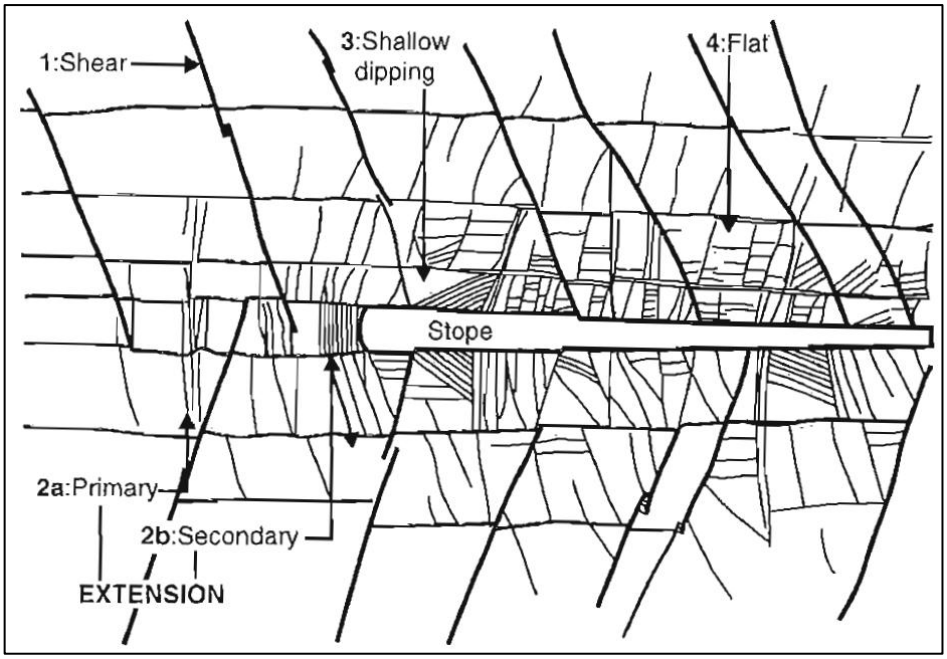


Figure 2.9: *Stress fractures around a deep stope mined in strong, brittle quartzite (Jager and Ryder, 1999)*

2.3 Key Debates and Controversies

Milev and Spottiswoode (2002) investigated the effect of rock properties on mining-induced seismicity in the Witwatersrand basin gold mines. The study included Mponeng Mine, where they concluded that the seismicity generated in the hard lava and quartzite footwall has no difference from the seismicity generated in the hard lava and Booysen Shale footwall. However, a clear difference in the seismic response between the two areas has been observed in this study. The current mine

design and support strategies do not recognise the difference in the seismicity and rock mass response between these two footwall zones.

Scheepers et al. (2012) indicated that the magnitude of a seismic event does not completely describe the potential for damage; however, the larger magnitude events have been found to have a higher potential for rock damage. The rock mass characteristics have also been found to play a huge role in the resultant damage. There are instances where smaller magnitude events have caused significant rock mass damage, while there are larger magnitude events with little or no damage. The quantity of damage at Mponeng Mine is influenced by the mechanical properties of the footwall rock mass rather than the magnitude alone.

Scheepers et al. (2012) highlighted the influence that the distance of the seismic event to the excavation face has on the extent of damage to the excavation. This means that the closer the event is to the excavation, the higher the potential of causing damage. This is true, however, more in a more brittle rock mass (quartzite footwall) than in the ductile rock mass (shale footwall).

Hofmann (2012) correlated the use of elastic modelling with the recorded seismic events at Mponeng Mine. This assists in the design of the stope profiles. Numerical modelling tools are an essential part of the design process, and they are extensively used to assess the stability and potential for seismic activity.

When preconditioning is effectively done, it relieves the stresses in the immediate face area, thus providing a safe working area (Modisha and Zvarivadza, 2015). Preconditioning is believed to improve the ground conditions of the panels. Thebethe (2018) researched the effectiveness of preconditioning at Mponeng mine. The study showed that the shale footwall panels have deeper fracturing than the quartzite footwall panels (Thebethe, 2018).

2.4 Chapter Summary

In this chapter, the key concepts, theories and studies were defined. The first step was to define the lithology of the Witwatersrand basin and Mponeng Mine. The challenges with each lithology were defined, and assumptions were discussed. The subject of seismicity and rockbursts was reviewed, and the sources of

seismicity were defined. The concept of ERR was defined, and its dependence on the stope convergence was discussed. The study demonstrated how the laboratory tests can be used to define the rock mass behaviour.

Previous studies suggested that the seismic behaviour is constant throughout the mine. This chapter has shown that a change in rock type can have a significant influence on the overall seismic behaviour.

3 RESEARCH APPROACH

3.1 Introduction

The research followed qualitative and quantitative research methods. The qualitative research compared the physical conditions in the sample workplaces. The quantitative research investigated the mechanical properties of the hanging wall and footwall rock samples taken from each footwall zone at Mponeng Mine. The seismic data and resultant damage were gathered for the same period.

3.2 Research Design

The research was designed to correlate the seismic distribution and associated observed rock mass damage to the mechanical properties of the intact rocks. The geotechnical zones were determined based on the mechanical properties of the intact rock. Working places were chosen in two representative geotechnical areas. The workplaces needed to be at about the same elevation and have a similar geometry and rate of mining. These workplaces were chosen to represent the ultimate stope design and configuration of the whole mine.

The physical conditions and seismic distribution within the chosen workplaces were studied. The contributing factors to the observed conditions and response to seismicity were investigated. The geomechanical properties were used in elastic numerical models to determine a correlation with observed damage.

3.3 Data Collection Process

3.3.1 Physical ground conditions

Underground visits were conducted to assess the physical ground conditions in the stopes of the East mine and the West mine. In particular, the following was assessed in both areas:

- the hangingwall and footwall fracture density;
- the face conditions; and
- the approximate closure in the working area.

Once the contrast in the stope ground conditions was understood, the observations were correlated to the observed damage.

3.3.2 Core sampling collection

The intact rock samples for the laboratory test were collected from diamond core drilling. The drilling was conducted for each zone from the footwall excavations through the reef into the hangingwall. This gave the solid core samples of the immediate footwall and hangingwall. The shale rock mass described as Zone A in Chapter 2 is laminated. The core drilling through the Zone A shale was aligned to intersect the strata perpendicular to the dip. This was designed to eliminate the influence of the laminations in the unconfined rock strength tests. The orientation of the holes through other rock formations was not crucial, as it did not affect the strength of the intact core.

3.3.3 Laboratory tests

The collected intact core samples were taken to the Wits Gold Fields Laboratories, where the uniaxial compressive strength tests with strain measurements and Brazilian tensile strength tests were conducted.

3.3.4 Seismic data

A seismic database was kept for the west and east mines. Using the Institute of Mine Seismology (IMS) Vantage software, the seismic events for the two raise lines were filtered to eliminate far-field events and geology structure-related events. The distance to the affected panels was also measured in Vantage.

3.3.5 Elastic Modelling

The determined mechanical properties of Booysen's shale and Kimberley quartzite were used in the Map3D numerical model to compare the results of closure and ERR.

3.4 Data Validation Process

Five samples of each rock type in the immediate mining vicinity were geomechanically tested in the laboratory. The testing aimed to determine if there was a correlation between observations and rock strength properties. Multiple samples allowed for a reasonable average to be determined. The data was also

validated against tests done by other researchers in the mining industry. The seismic data was validated with the monthly seismic database kept at Mponeng Mine. The observed trend in the two selected raise lines corresponded with the overall mine trend for each geotechnical zone. This validated that the analysis of these two raise lines represented the whole geotechnical zone.

3.5 Data Analysis Approach

The data analysis was conducted by first defining the mechanical properties of each rock type in each footwall zone at Mponeng Mine. The properties were used to define the geotechnical zones. The mechanical properties were used as input parameters in a Map3D numerical model. This was done to determine the distinctive behaviours of each rock mass. The differences were compared to physical stope conditions observed from underground assessments and then correlated to the differences in seismic response of each area.

Only the burst-type events were selected for the study as they relate to the stope faces and the stress distribution ahead of the faces. The seismic distribution between the two areas will be compared between the sample raise-lines in each geotechnical zone. This will show which area has the most large-magnitude seismic events. The damage resulting from seismicity within these workplaces was compared to demonstrate which area suffers the most damage. The number of large-magnitude seismic events was also correlated to the amount of damage. The study subsequently investigated the factors that influenced the observed seismic activity. The resultant damage was compared to the mechanical properties of the surrounding rock mass.

3.6 Chapter Summary

The chapter began by describing how the research was designed. The data collection process was defined. This included the investigation of the physical underground conditions, collection of the intact rock samples and laboratory testing, seismic data analysis and the use of the mechanical properties of the intact rock in numerical modelling. The data validation steps and analyses were defined.

4 DATA FOR THE STUDY

4.1 Introduction

This chapter will show the observed underground physical conditions of each geotechnical zone. The laboratory test results will also be given in this chapter. The seismic response of both geotechnical zones will be defined, and the total volume of investigated damage will be quantified. The mechanical properties of the host rocks will explain the observed damage. The numerical modelling results from the Map3D software will be presented in this chapter.

4.1.1 Underground observations

Visits were conducted to relevant panels on the East and West mine, where the footwall is Booysen's shale and quartzite, respectively. The stope layout (panel length and lead/lag) is the same in both footwall zones. The physical conditions of the rock mass in the panels were recorded to determine any difference in physical appearance in areas unaffected by a seismic event. The differences were recorded and analysed to determine possible reasons for the differences. Four raise lines were visited (**Figure 4.1**), two in each area of interest. The two raise lines in the area with Booysen's shale footwall (East mine) were 113/67 and 120/66. The two raise lines in the area with quartzite footwall, Kimberley quartzite and Elsburg/Denny's quartzite, were 123/51 and 120/33 raise lines.

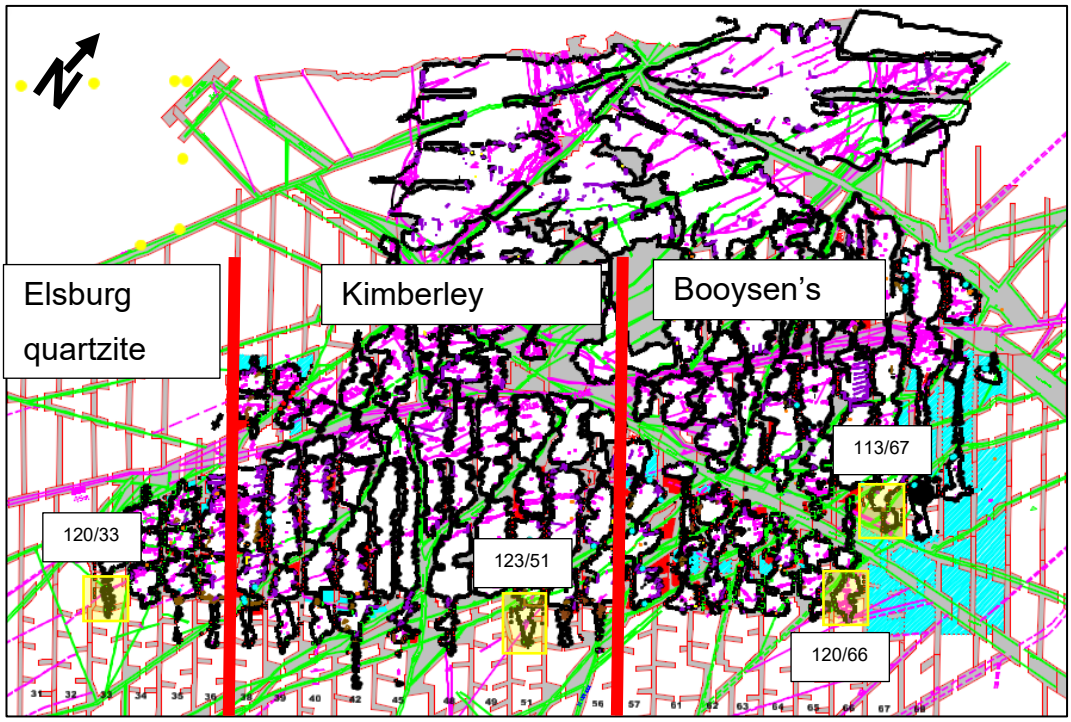


Figure 4.1: *Macro plan view of Mponeng mine showing the position of the visited stopes (120/33, 123/51, 120/66 and 113/67)*

Face perpendicular preconditioning is one of the methods used at Mponeng Mine to reduce the face stresses (Thebethe, 2018). The preconditioning also reduced the impact of rock bursts (Modisha and Zvarivadza, 2015) and created safer work face conditions. The same preconditioning standard is maintained throughout the mine with a maximum hole spacing of 3.0 m and a hole depth of 2.4 m. The depth of fracturing in the section of the shale footwall is deeper than in the quartzite footwall (Thebethe, 2018). This can be a contributing factor to the good ground conditions observed in the stopes in the shale footwall. The assessment using the Ground Penetrating Radar (GPR) in the stopes of both footwall zones indicated sufficient depth of fracturing in both areas, more than was found during the GAP 336 project (Thebethe, 2018). This concluded that there are no issues with the current preconditioning standards and practices at Mponeng Mine in both the quartzite and shale footwall zones. The observed ground conditions in the sections below are more influenced by the mechanical characteristics of the rock types, as the same preconditioning was applied in both areas.

4.1.1.1 East Mine

A couple of panels were visited in each raise line to determine the general conditions of the stope-hangingwall. The hangingwall lava was observed to be porphyritic. Some amygdales and calcite vugs were observed on the surface of the hangingwall. However, in general, the hangingwall lava was massive from a few centimetres above the hangingwall contact. Core specimens were collected from the diamond exploration hole that was drilled at 123/61 raise-line. The core started in Krugersdorp quartzite and extended through the Booysens shale, VCR and into the hangingwall lava. Mostly, the core samples showed a massive lava type with few amygdales.

At 113/67, the hangingwall lava was sandy and included weak calcite pebbles. The hangingwall in the East mine generally looked smooth and flat (**Figure 4.2**). The footwall conditions also look flat and smooth, making the support installation easy (**Figure 4.3**). The hangingwall had shear fractures, joint planes and face parallel fractures. No wedge failures were observed in these panels. The support installation is easy, and the ground conditions are stable.



Figure 4.2: *Photos from different stopes showing the generally smooth hangingwall conditions in the east mine stopes*



Figure 4.3: *Smooth footwall conditions created by the soft shale rock mass*

4.1.1.2 West mine

Two raise lines were visited on the West Mine, where the footwall was Elsburg/Denny's or Kimberley quartzites. Most of the immediate hangingwall had a high percentage of amygdales, but became massive a few tens of centimetres

into the hangingwall. Hangingwall lava specimens were collected from a borehole drilled at 123/35 from the Elsburg/Denny's quartzite footwall zone. Other samples were collected from a borehole drilled at 123/39, which is in the Kimberley quartzite footwall zone. The samples collected at 123/35 in the Elsburg/Denny's quartzite footwall zone will be referred to as Far West, whereas the specimen from 123/39 in the Kimberley quartzite will be referred to as the West specimens.

The physical conditions of the hangingwall in the West of the mine were undulating with many fractures and brows (**Figure 4.4**). The hangingwall was affected by the shear fractures, joint set frequency, blasting fractures and face parallel stress fractures, which affected the stability. The hangingwall was significantly more fractured than on the East mine. The footwall conditions are also highly fractured and undulating (Figure **4.5**). Support installation was more difficult, resulting in strata control challenges.



Figure 4.4: *Photos from different stopes showing the uneven hangingwall conditions in the west mine stopes*



Figure 4.5: Uneven footwall conditions created by the hard and brittle quartzite rock mass

4.2 Mine plan observations

When assessing the mine plan, it indicates that from the planned block of ground to be mined, there is a higher percentage of the ground lost in the western stopes in quartzite footwall than in the eastern stopes in the shale footwall. This loss of ground excludes the losses due to the geological structures. The most loss has been observed in the lagging panels as they are the last panels to mine up to the dip pillar position. As the panels mine in line, the stress lobe ahead of the stopes increases, which increases in seismic response ahead of the profile. The rockburst damage caused by these seismic events results in the loss of ground. About 90% of panels last two panels in the quartzite footwall raise lines do not mine up to the dip pillar position, stopping between 10 – 20m from the dip pillar position.

Figure 4.6 below is a good example where the top panel of the 116/65 raise in the shale footwall is compared to the top panels of the 116/35 raise in the quartzite footwall. The planned mining area at the top of 116/65 raise is calculated to be about 21 576m^2. The bottom 3 panels were stopped after a seismic event ahead of W6 resulted in the damage of W6 gully and siding (purple circle in Figure 4.6 (a)), fatally injuring one employee. The area of the stopped panels is calculated to be about 1500m^2, which is about 7% loss. On the other hand, the planned mining area at 116/35 top is calculated to be about 21 924m^2. The top two panels to the east were stopped after a seismic event ahead of the E8 panel (purple oval in Figure 4.6 (b)) caused damage at the bottom of the panel, which fatally injured one employee. The bottom two panels to the west were stopped due to the increased seismic activity along the small dyke, which resulted in damage along the faces. The total ground lost is about 2020m^2 which is about 9% loss. This trend is

consistent in most raise lines in the quartzite footwall, where the last two panels in a profile cannot be mined up to the dip pillar position.

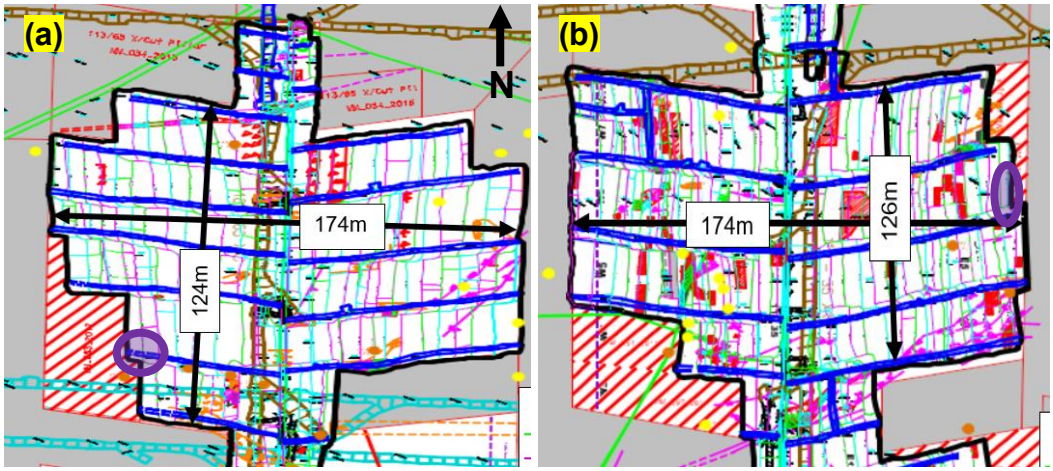


Figure 4.6: Top block of 116/65 raise (a) in shale footwall and 116/35 raise (b) showing the loss of ground with red hatching due to rockburst or increase in seismic activity ahead of the stopes

4.3 Rock Strength Properties

Laboratory intact rock strength tests were done on rock samples collected from the diamond drill core in the two geotechnical zones. Five core samples were collected from each of the two footwall rock types and the hangingwall of the different footwall zones. Uniaxial compressive strength tests with modulus (UCM) were conducted as per the methodology described in the ISRM (1981).

4.3.1 Uniaxial Compressive Strength Results

The compressive strength, Young's Modulus (E) and Poisson's ratio (v) are important parameters in rock engineering design (Armaghani et al., 2014). All the uniaxial compressive strength tests were conducted with strain measurements so that the Young's Modulus and the Poisson's ratio could be calculated. The results from all the conducted tests, including the resultant Young's Modulus and Poisson's ratio, are presented in Appendix A.

4.3.1.1 UCS results

The compressive strength results show that the lava hangingwall is almost constant throughout the mine (**Figure 4.7**). Even though there are a few

characteristics of lava that are different in each area, they do not significantly affect the compressive strength of the lava. The strength variation of the footwall is, however, much greater. The Booysens shale footwall has the least strength of all the footwall types, with the Kimberley quartzite having the highest strength figure (**Figure 4.7**). Both lava and quartzite fail in a brittle manner by creating multiple fractures as observed in the unconfined rock tests. The shale rock also presented some brittleness as it still contains some quartz minerals (Ye, Tang, Xi, et al., 2024); however, the high level of creep failure made it less violent.

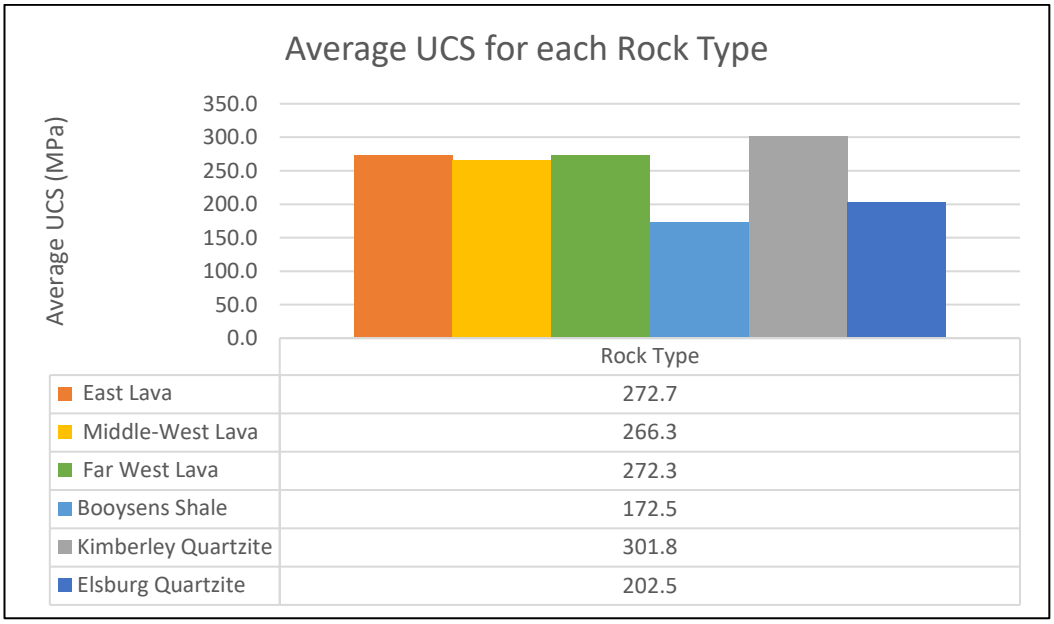


Figure 4.7: *Plot of the average UCS values for each rock type specimen found in the three zones at Mponeng Mine*

4.3.1.2 Young's modulus results

Young's modulus is defined as the ratio of stress to strain. It is calculated from the gradient of the elastic zone of the stress-strain graph. The higher Young's modulus value means the material develops more stress for a smaller deformation. Strong, brittle rock materials often have a higher Young's modulus than soft, ductile materials (Chang et al., 2006). From the Young's modulus plot of the hangingwall lava and footwall rocks from the three footwall zones, the lava hangingwall is the strongest and likely the most brittle rock mass. The eastern lava has the highest Young's modulus (**Figure 4.8**). Comparing the footwall rock masses, Kimberley quartzite has the highest Young's modulus, suggesting that it is the most brittle

footwall rock mass. The Booysens shale, on the other hand, has the lowest Young's modulus, meaning that it deforms more before failure.

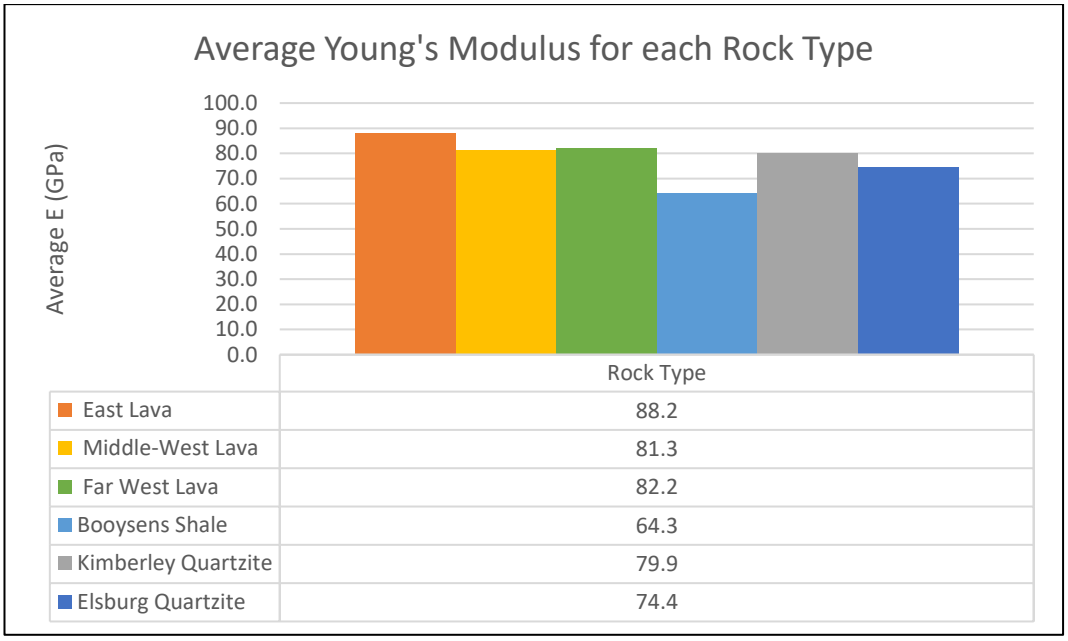


Figure 4.8: *Plot of the average calculated Young's Modulus result for each rock specimen found in three footwall zones at Mponeng Mine*

4.3.1.3 Poisson's ratio

Poisson's ratio is defined as the ratio of lateral strain to axial strain. The higher Poisson's ratio value means that the material has a greater expansion in the direction of the minor principal stress than a material with a lower Poisson's Ratio. The Poisson's ratio results are shown in **Figure 4.9**. The shales have the highest lateral strain during loading.

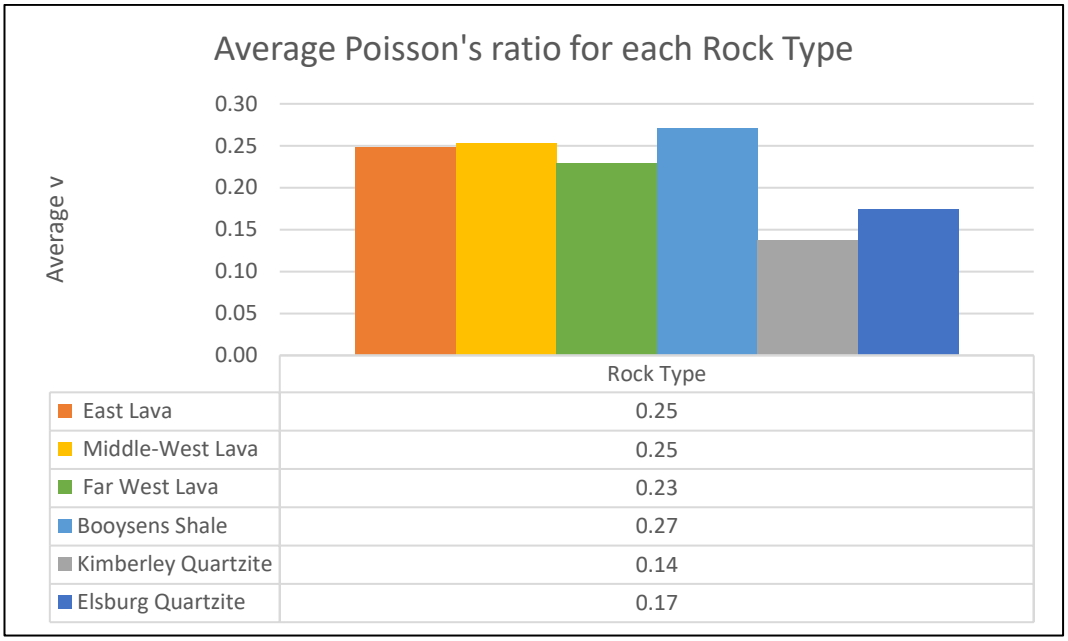


Figure 4.9: *Plot of the average calculated Poisson's ratio result for each rock specimen found in three footwall zones at Mponeng Mine*

4.3.2 Numerical modelling results

The available numerical modelling package was a boundary element, elastic model, which cannot show the influence of different rock properties. For this exercise, two models of the same area were run with the material properties of the shales as per the intact rock test results of the Booysen's shale and the other with the intact rock test results of the Elsburg quartzite. The model was done to compare the closure results. **Figure 4.10** show a comparison of the closure results from the model. The results showed that the shale footwall has a higher closure result than the quartzite footwall, as expected and observed underground. The underground observations have shown that the higher closure rates in the shale are mostly from the footwall heave. In some raise lines, total closure has taken place in the stopes, and it is evident that the footwall has heaved more than the hanging wall closure. The observed lower fracturing in the hangingwall can be explained by lower stress in the immediate face due to the footwall punching. The high stress is therefore transferred further ahead of the face, where the confinement is higher. The smaller number of fractures results in improved hangingwall conditions and fewer FOGs during a seismic event.

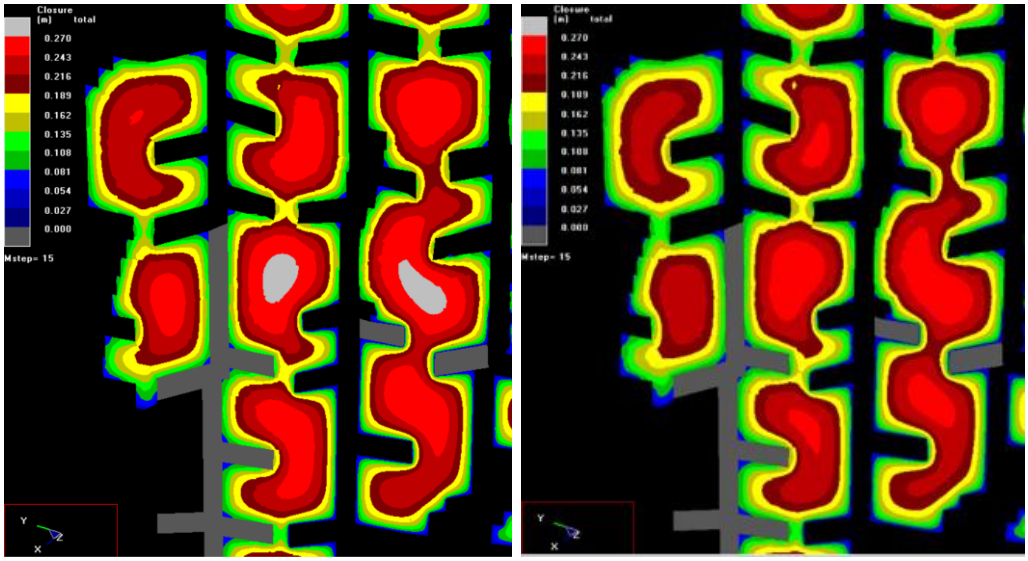


Figure 4.10: *Map3D numerical closure modelling results of the same area using the Shale properties (left) and quartzite properties (right)*

As indicated earlier, ERR is directly proportional to convergence. The shale footwall zone has higher convergence and therefore a higher ERR. An area was selected and modelled first with shale properties and again with quartzite properties to demonstrate the difference in ERR results. The modelled ERR results below correlate with the closure/convergence results, with the shale properties having higher ERR values (**Figure 4.11**).

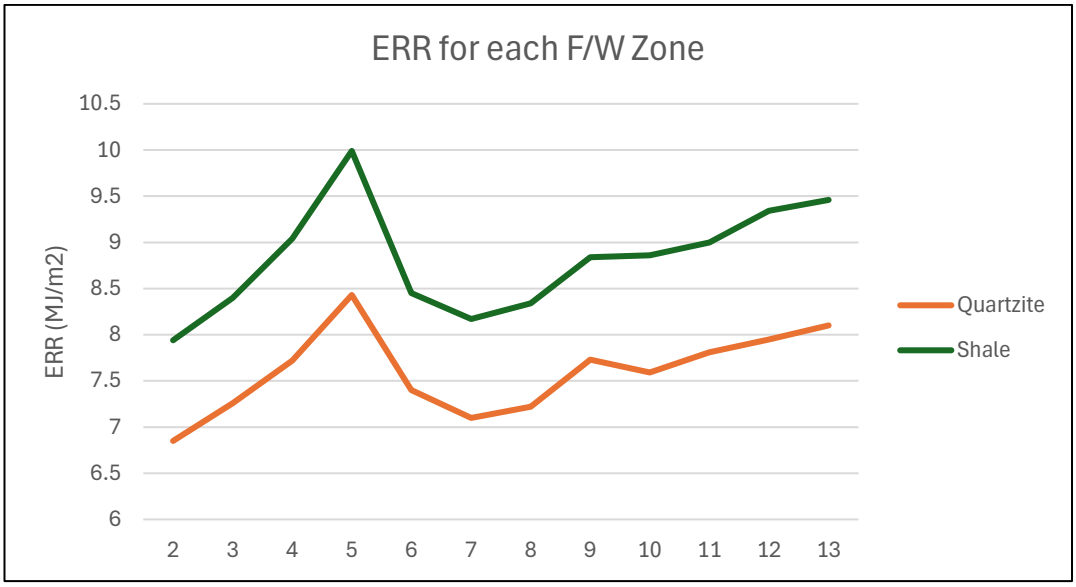


Figure 4.11: *Modelled ERR results using the shale and quartzite mechanical properties*

The difference in ERR results was not as significant as one would expect. Smaller-magnitude events in the shale footwall zone are located further ahead of the face, where the rock mass is solid and accumulates stress. The smaller-magnitude events in the quartzite footwall zone are located close to the face due to the hardness of the quartzite, which accumulates stress more easily. The poor ground conditions created by the brittle quartzite and hard lava exacerbate the rockmass damage during a rockburst event.

4.4 Seismic Response

Several factors influence the seismic response to mining. These include geological structures, mining spans, face configuration, and the rock type. This makes it very difficult to compare the two footwall zones. To compare the seismic response and the resultant damage due to the rock type, it is necessary to eliminate all the other influencing factors. Only two areas could be assessed, one in Booysen's shale footwall and one in the quartzite footwall, where the mining geometry, geological structures and mining depth were similar. The 116/65 and 116/35 raise lines were chosen for this comparison, where mining was 3154 m to 3254 m below the surface.

4.4.1 116/65 and 116/35 geological and geometrical comparisons

There are two major geological structures close to the 116/65 raise line. The Georgette South dyke north of the raise strikes E-W, and a minor EE dyke offshoot west of the raise-line, striking from NE-SW. Both dykes are included in the 20 m bracket pillar, which does not contribute much to the seismic activity in the workplace. Multiple small faults are intersected in the eastern panels, striking in the NE-SW direction. The bottom two western panels were prematurely stopped after a fatal accident in October 2017. The average dip and strike span are measured to be 124 m by 174 m (**Figure 4.12**).

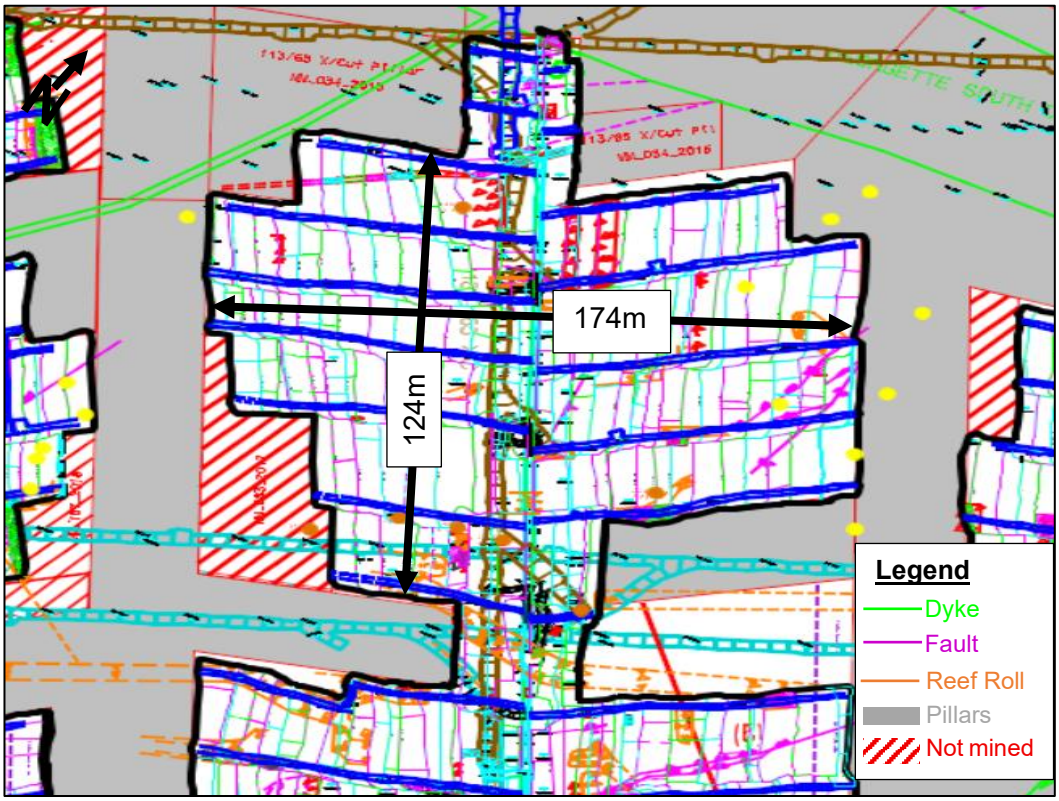


Figure 4.12: *Plan of 116/65 (Booysen's shale footwall) showing the geometry of the mined-out area and the nearby geological structures.*

There are no large geological structures close to the 116/35 raise line. There are, however, two small dykes intersecting in the western panels, one striking in the N-S direction while the other is striking in the NE-SW direction in the W4 panel. Multiple faults are intersected in the E4 panel. The bottom western panels were

also not mined to the dip pillar position due to poor ground conditions. The dip and strike span is measured to be 126 m by 174 m. The top two eastern panels did not mine to the dip pillar position due to poor ground conditions (**Figure 4.13**).

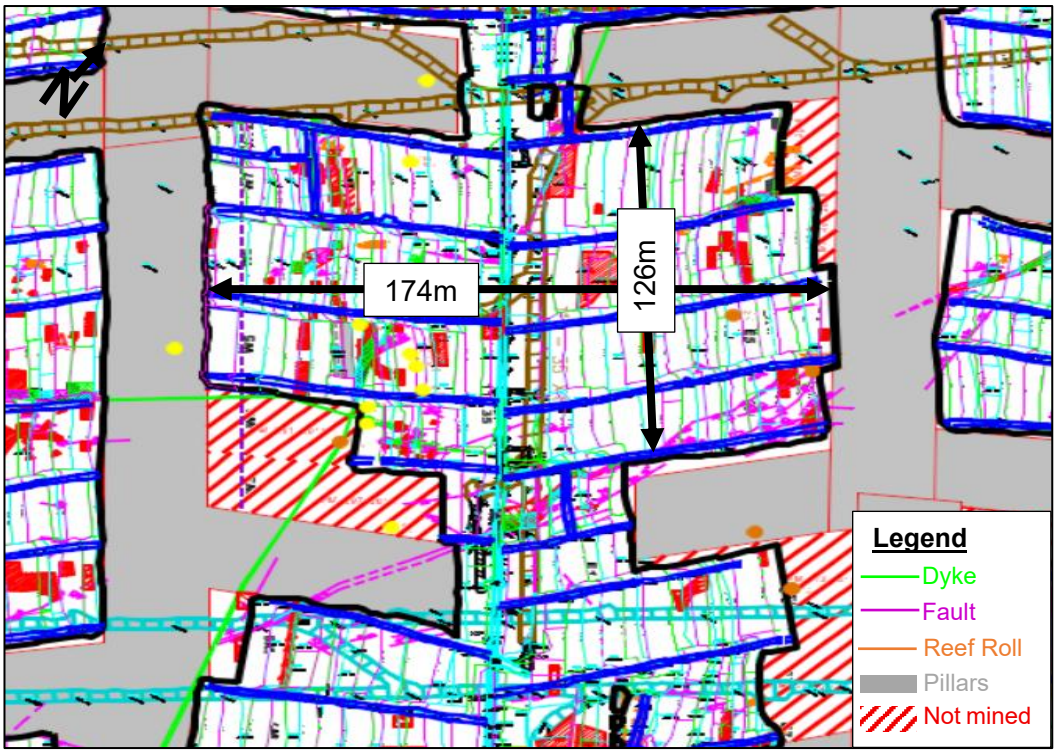


Figure 4.13: *Plan of 116/35 (quartzite footwall) showing the geometry of the mined-out area and the nearby geological structures.*

4.4.2 Seismic comparison between 116/65 and 116/35 raise lines

Both raise lines were mined during the same period and are positioned at the same depth; therefore, they have the same virgin stress state. This report only focuses on the 2017 to 2018 period, where the production was almost at the peak for both raise lines. Only events with a magnitude greater than 1.0 were considered for the analysis, as they can result in a rockburst.

From all the recorded events in the two raise-lines over the two years (**Figure 4.14**), it indicates that there was much more damage reported in the 116/35 raise-line than in the 116/65 raise-line. Though 116/65 raise-line had a total of 35 events in the two years compared to 27 events in 116/35, the total amount of seismic

damage is more than 3 times the size of the observed and investigated damage at 116/65. The amount of damage was quantified from the measured damage during the fall of ground investigations. The fall of ground database is kept at Mponeng Mine's server as a Microsoft Word report and a Microsoft Excel spreadsheet. The database of all the falls of ground investigations shows that the observed damage trend applies in both geotechnical zones, i.e. the west mine has fewer large magnitude events but larger areas damaged and vice versa. The question is, however, are these events the same?

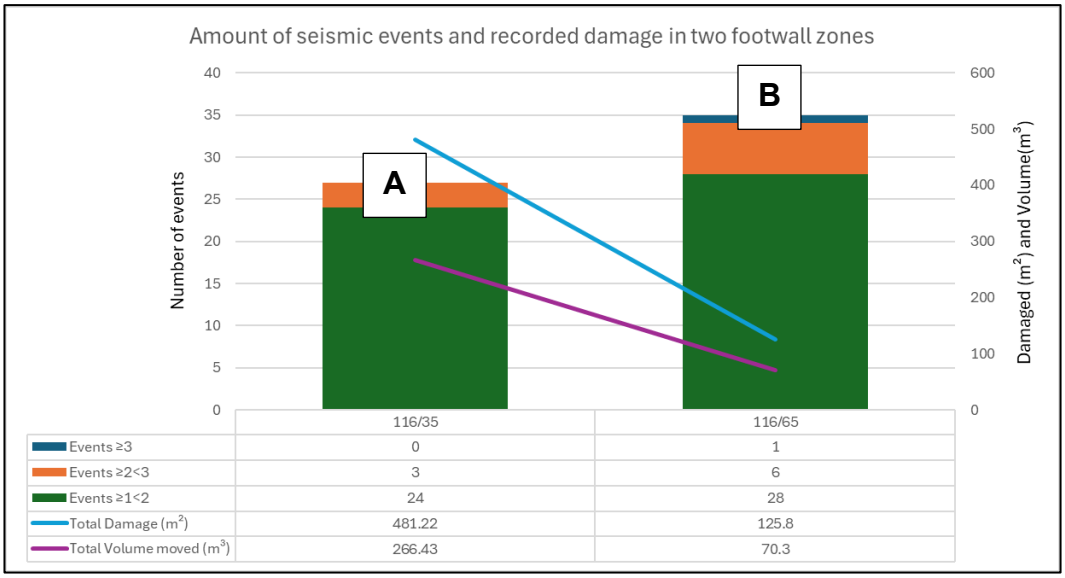


Figure 4.14: *Number of seismic events with ML≥1.0 per raise-line for each year, with the total investigated rock mass damage. A=Quartzite Footwall, B=Shale Footwall*

The event clustering in both raise lines in 2017 and 2018 raise lines is demonstrated in **Figure 4.12** and **Figure *4.13*** with brown and yellow dots, respectively. At 116/65, the 2017 events clustered more around the W2 panel, but the 2018 events clustered more along the eastern dip pillar and 116/64 eastern panels. At 116/35, the 2017 events cluster around the eastern panels, while in 2018, the events cluster around the western panels, more around the W4 and W5 panels. The area has several geological structures, but based on the moment-tensor decomposition analysis, most of the events are burst-type events, which are face-related. The moment tensor analysis of the seismic events at 116/65 shows that most of those events are slip-type events related to some geological structure

rather than the burst-type events, which are related to the face or abutment failure. Even though there were more slip-type events, which usually have a higher magnitude and energy, there was minimal damage in the panels. When eliminating these slip-type events, the amount of large magnitude events in the shale footwall decreases, as will be demonstrated later in Chapter 5.

4.5 Chapter Summary

The general physical ground conditions for each geotechnical zone were determined in this chapter. The hangingwall in the quartzite footwall (West Mine) was significantly more fractured than in the shale footwall (East Mine). The quartzite footwall was also highly fractured and undulating. It should be noted that it is highly unlikely that the hangingwall fracturing is impacted predominantly by the footwall rock type. The virgin stress-UCS ratio for Shale is (85/172 = ~50%), which would equate to extreme fracturing of the footwall, and for the Lava it is 30%, which is where fracturing commences. The shale footwall, however, flows instead of fracturing and is more prone to creep, which reduces fracturing in the hangingwall. The quartzite footwall has a higher propensity for fracturing. At mining-induced field stress levels, the hangingwall is expected to be highly fractured, except if the face is de-stressed (pre-conditioning or over-stoping). Preconditioning in both footwall zones is effective; however, the deeper fracture distance in the shale footwall contributes to the better ground conditions observed in shale footwall stopes.

It was proven that the laboratory intact rock strength test results from the rock samples taken from each footwall zone show that both the lava and quartzite are very strong rocks with relatively low tensile strength and high modulus. The low Poisson's ratio demonstrates its inability to expand; therefore, it is brittle.

The laboratory intact rock strength test results of the rock samples taken from the East mine show that the lava has high compressive strength while the shale is weaker. The 116/65 raise-line in the eastern mine has shown to have more large magnitude seismic events than seen at 116/35 raise-line in the western mine. Though there is a larger number of seismic events, there is far less damage caused by these events at 116/65 raise-line representing the eastern mine compared to the observed damage at 116/35 raise-line representing the western mine. Though

this was only done in single raise lines in the two footwall zones, the same trend has been observed across all raise lines in each corresponding footwall zone.

5 ANALYSIS AND FINDINGS

5.1 Mechanical properties of intact rock

The lava has a constant compressive strength throughout the mine; therefore, it cannot be the main contributor to the difference in the rock mass behaviour in these footwall zones. The observations from the laboratory tests have shown that the lava is brittle. The high Young's modulus and low Poisson's ratio indicate the inability to heave or yield, suggesting brittle behaviour.

All the laboratory tests demonstrated that the quartzite footwall material is brittle. The hardness of the mineral causes the quartzite rock to be brittle. The high Young's modulus and low Poisson's ratio indicate the inability to heave or yield, suggesting brittleness. The laboratory test results demonstrated that the quartzite has a high Young's modulus (79.9GPa) and a low Poisson's ratio (0.14), indicating that it is a brittle rock. As both rock masses are brittle, they result in highly fractured rock conditions both in the hangingwall and footwall, as determined earlier in the underground observations. As a result of severe fracturing of the hangingwall and footwall, the rock mass easily fails during the dynamic loading caused by the seismic event.

The Booysen's shale had a lower Young's Modulus (64.3GPa) and a higher Poisson's ratio (0.27). These results suggest it could absorb comparably more strain energy and yield more easily. Since the shale is in the footwall, the hangingwall damage or failure is minimal, but there is more footwall heave. The hangingwall becomes less fractured and more competent, which explains why there is less rock mass damage in the east mine.

5.1.1 Intact rock strength

The intact test results of the rock samples taken from the East Mine show that the lava has high compressive strength and is brittle. The shale has lower compressive

strength and is ductile. The combination of the two rock masses means that the shale absorbs more strain energy, which creates overall good ground conditions.

The intact test results of the rock samples taken from the West Mine show that both the lava and quartzite have high compressive strength and are brittle. They are both incapable of absorbing the strain energy. This leads to the propagation of fractures into the hangingwall and footwall. The inability to absorb the strain energy results in the generation of burst-type events along the face and abutments.

5.1.2 Rock mass strength

The intact rock strength does not define the strength of the rock mass. The Hoek-Brown failure criterion (Hoek and Brown, 2019, 1980a) was used to plot the failure envelopes of these rock masses at fixed minor principal strength values to understand the rock mass behaviour. Since the intact rock specimens were used for the σ_{ci} values, the m_i constant will be estimated for the calculation based on the table in the Hoek and Brown (1997) paper. The estimated m_i constant and calculated results are shown in **Table 5.1**.

Table 5.1: *Estimated m_i values for each rock type and the calculated σ_1 value for each fixed σ_3 value*

AVERAGES	UCS	E	ν			East Booysens Shale	East Lava	West Lava	West Kimberley Quartzite FW	Far West Amygdaloidal Lava	Far West Elsberg Quartzite
	(MPa)	(GPa)		m_i	σ3	σ1					
East Booysens Shale	172.5	64.3	0.27	9	0	172.54	272.73	266.27	301.77	272.33	202.52
East Lava	272.7	88.2	0.25	17	5	198.74	317.35	310.83	361.76	316.95	260.58
West Lava	266.3	81.3	0.25	17	10	222.84	357.49	350.83	414.34	357.08	309.37
West Kimberley Quartzite FW	301.8	79.9	0.14	24	15	245.35	394.38	387.55	461.88	393.96	352.53
Far West Amygdaloidal Lava	272.3	82.2	0.23	17	20	266.63	428.79	421.78	505.71	428.36	391.79
Far West Elsberg Quartzite	202.5	74.4	0.17	24	25	286.90	461.23	454.03	546.66	460.78	428.15
					30	306.33	492.03	484.64	585.29	491.58	462.24

The Hoek-Brown failure envelopes for the Booysens shale footwall zone, Kimberley quartzite footwall zone and Elsburg quartzite footwall zone are shown in **Figure 5.1**. The figure shows that the Booysens shale is the least competent rock mass. Kimberley quartzite rock mass is the most competent. The strength of the lava rock mass is almost constant across the mine, and it is stronger than the Elsburg quartzite.

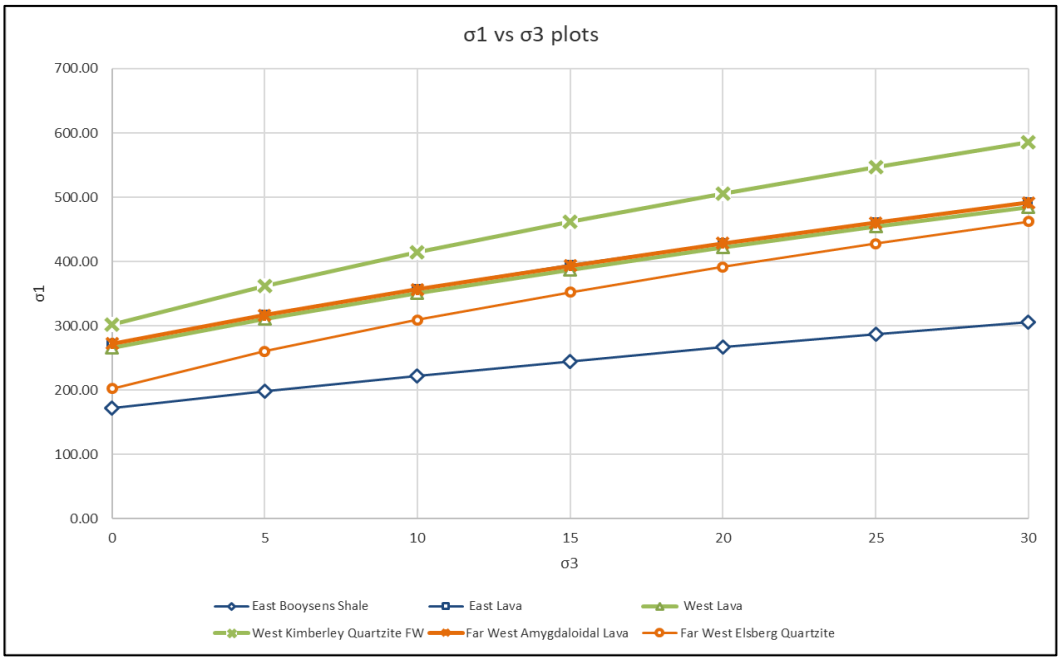


Figure 5.1: *The σ_1 vs σ_3 plot based on the Hoek-Brown failure criterion for each rock mass encountered at Mponeng Mine*

The consistency in the rock mass strength of the lava hangingwall across all geotechnical zones suggests that the hangingwall is not the main influence on the rock mass failure. There is, however, a significant variance in the strength of the footwall rock masses. The variance in the strength of the footwall is likely to be the reason for the difference in the rock mass behaviour during a seismic event. The question one should ask is: why is there more hangingwall damage from the smaller magnitude seismic events in the west mine, even though the hangingwall rock mass strength is almost constant throughout the mine?

The underground observed closure is higher in Booysen's shale as the footwall has higher heaving. Some old stopes in the Booysen's shale have total closure, which shows that there is generally higher closure in the shale than in the quartzite. The quartzite footwall is comparatively more brittle, causing both the hangingwall and footwall to fail almost simultaneously, resulting in both hangingwall and footwall being highly fractured. The lava hangingwall indicates to have high strength with a bit of ductile properties indicated by the high Poisson's ratio, while the quartzite is more brittle as it has high Young's modulus and low Poisson's ratio (**Figure 5.2**). The Booysen shale is the most ductile of the rock formations, as

indicated by the lowest Young's modulus and the highest Poisson's ratio (**Figure 5.2**).

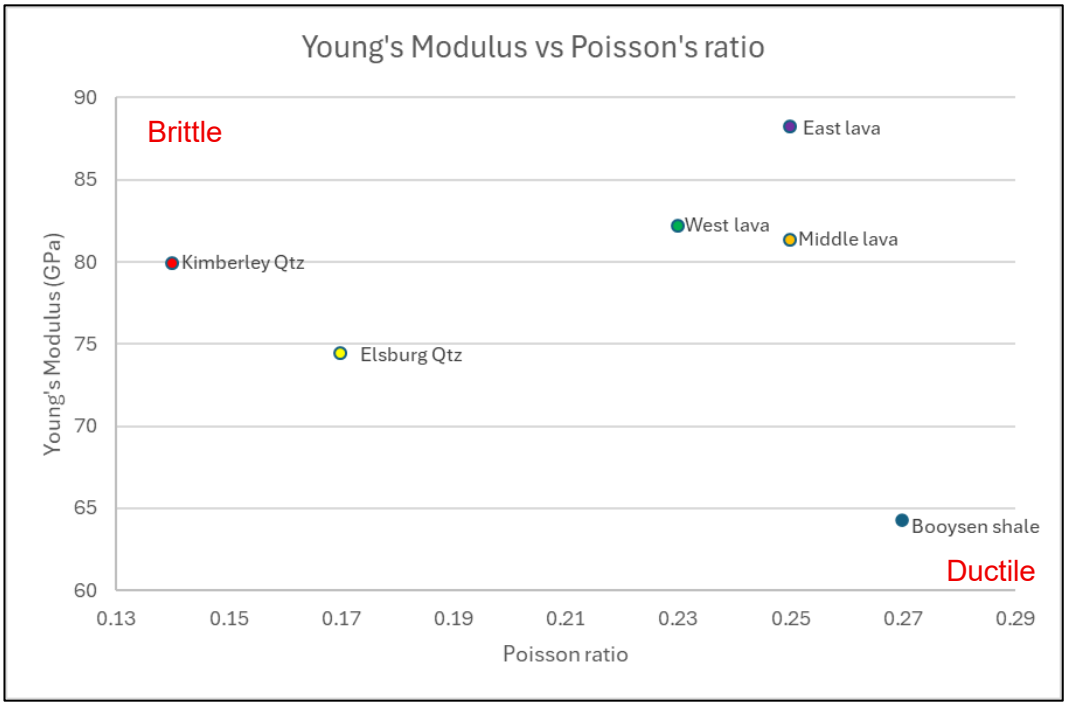


Figure 5.2: *A plot of Young's modulus and Poisson's ratio from the lab tests*

5.2 Seismic response

In the results section, it was determined that there is generally more damage from the raise line in the quartzite footwall zone than in the shale footwall zone. Analysing the seismic events further, **Figure 5.3** below shows that there are more burst-type events in the raise-line in quartzite footwall rather than in the raise-line in the shale footwall. The high-strength properties of quartzite rock mass contribute to the number of burst-type events that result in rock burst failure. The total production in the 116/35 raise-line in the quartzite footwall is less than in the 116/65 raise-line, but has resulted in a higher number of face-related events.

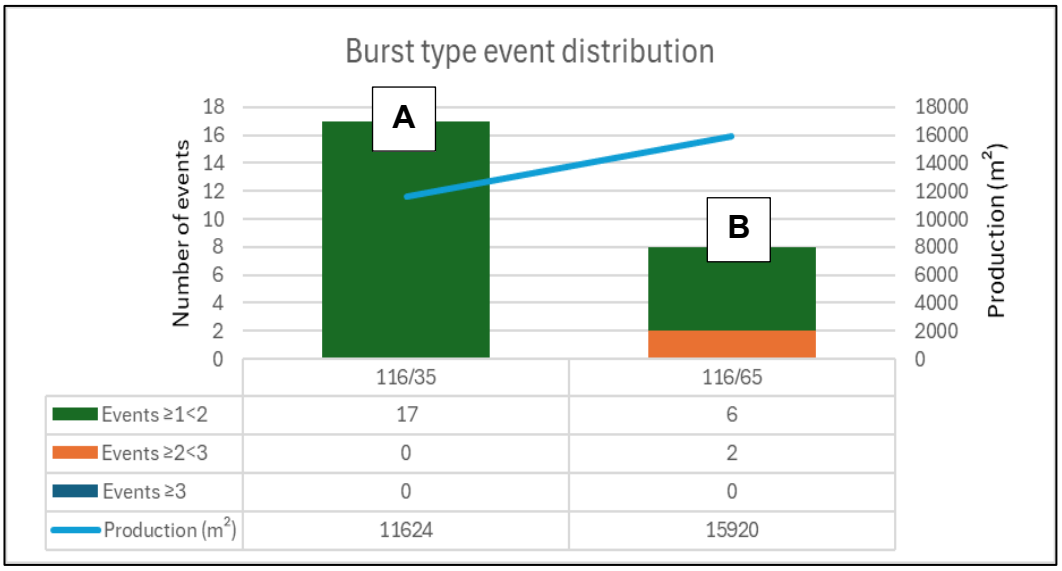


Figure 5.3: *Total burst-type events recorded in the 116/65 raise-line vs in the 116/35 raise-line. A=Quartzite Footwall, B=Shale Footwall*

The burst-type events in the quartzite footwall zone are located closer to the stopes than the shale footwall zone (**Figure 5.4**). This explains why most of the events in the quartzite footwall will result in damage rather than in the shale footwall. The stress accumulates along the face and abutment due to the hard quartzites, resulting in burst-type failure. The shale does not allow for stress build-up, therefore having a lesser burst-type failure. There are more slip-type events along the discontinuities in the shale footwall zone. Another interesting observation is that the burst-type events in the shale footwall have large magnitudes compared to the magnitudes recorded in the western stopes in the quartzite footwall. During dynamic loading from a seismic event, Booysen's shale footwall is observed to heave more. The shale footwall absorbs more energy through heaving than the brittle quartzite rocks. This explains why there is more damage on the western part of the mine in the quartzite footwall, even though the average magnitude of seismic events is smaller than on the eastern part of the mine.

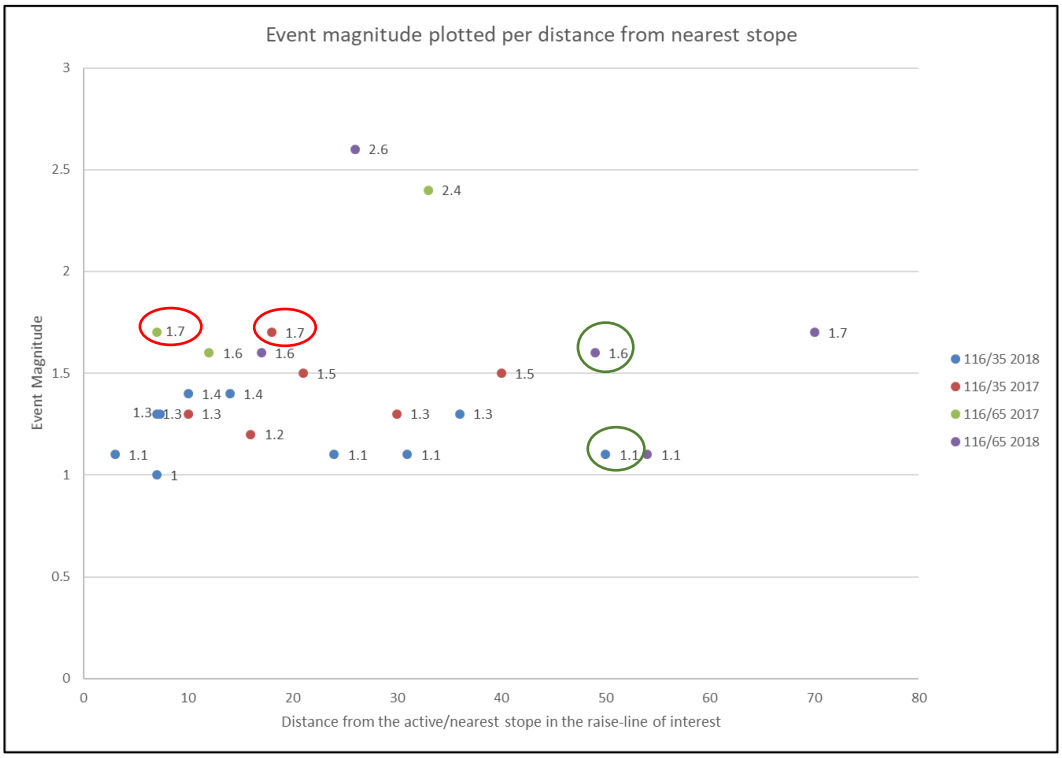


Figure 5.4: *Location of burst-type events to the active panels or the nearest panel in the raise-line of concern*

The higher closure and ERR in the shale footwall require higher stress to generate a burst-type seismic event, resulting in a higher magnitude event. Though the burst-type seismic events in the shale footwall zone are of higher magnitude (**Figure 5.4**), they don't result in as much rock-burst damage (**Table 5.2** and **Table *5.3***).

Table 5.2: Damage comparison caused by the seismic events of the same magnitude but at different distances

Event information	116/65 W2	116/35 E4
• Footwall type	• Shale	• Quartzite
• Event magnitude	• 1.7ML	• 1.7ML
• Event date	• 16 May 2017	• 4 July 2017
• Distance to panel (2D)	• 7m	• 18m
• Damage (Yes/No)	• No	• Yes
• Damage area and Volume	• 0	• 25.2m^2 and 32.76m^3

Table 5.3: Damage comparison caused by the seismic events with different magnitudes but at similar distances

Event information	116/65 W4	116/35 E6, E7
• Footwall type	• Shale	• Quartzite
• Event magnitude	• 1.6ML	• 1.1ML
• Event date	• 15 January 2018	• 6 February 2018
• Distance to panel (2D)	• 49m	• 50m
• Damage (Yes/No)	• No	• Yes
• **Damage area and Volume**	• 0	• 49.3m^2 and 14.79m^3

The 1.7 ML events were selected to compare the quartzite to the shale footwall. These events are highlighted with red circles in **Figure 5.4** and the results are summarised in **Table 5.2**.

The two events had slight differences in distance; however, the event that did not cause damage at 116/65 was even closer to the panel than the one that resulted in damage at the 116/35 E4 panel. This shows that the shale footwall absorbed most of the energy and did not cause damage to the rock mass. However, in the

quartzite, all the energy from the seismic event resulted in damage to the rock mass. A comparison was also made for the events with a similar distance to the panel face, and two events were circled in green in **Figure 5.4**. The damage results are summarised in **Table 5.3**. The larger-magnitude event closer to the 116/65 W4 panel in the Shale footwall did not result in damage, while the smaller-magnitude event located at a similar distance to the 116/35 panels in the quartzite footwall resulted in damage in two panels (i.e. 116/35 E6 and E7 panels).

The comparison in **Table 5.2** and ***Table 5.3*** indicates the typical response in the two footwall zones. Stopes in the quartzite footwall zone tend to suffer more damage than in the shale footwall zone, irrespective of the seismic event magnitude and/or distance to face.

5.3 Ground conditions

5.3.1 Stress fracturing

The lava hangingwall and the quartzite footwall found in the western part of the mine are both strong and brittle rock types. According to Jager and Ryder (1999), fracturing around a stope in a similarly strong and brittle hangingwall and footwall, the stress fractures propagate into the hangingwall and footwall (**Figure 5.5)**. This is suspected to be the reason why the hangingwall and footwall in the western part of the mine have more pronounced fractures. These fractures form unstable wedges (Jager and Ryder, 1999; Ryder and Jager, 2002) which makes the rock mass prone to failure between support units during seismic shake-downs. This is suspected to be the reason why there is more damage on the western part of the mine, even from smaller magnitude events.

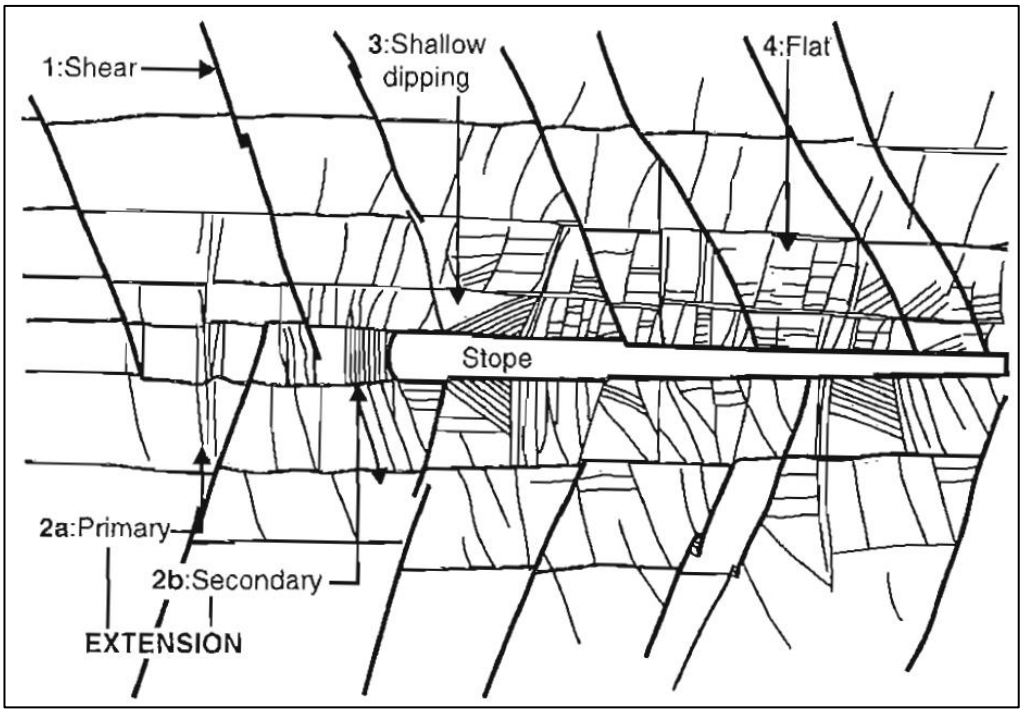


Figure 5.5: *Stress fractures around a deep stope mined in strong, brittle quartzite (Jager and Ryder, 1999)*

The softer shale footwall absorbs some of the face stress due to creep. This theory suggests that high stress is transferred deeper into the face under higher confinement conditions. Fracturing under such conditions is more likely to be in shear and spaced further apart. The hangingwall conditions in the eastern part of the mine are less fractured, as shown by the observations. The hangingwall is easier to support, and even during the vibrations caused by a seismic event, there is limited fallout. There are fewer unstable wedges formed in the hangingwall, which can fail between the installed support.

5.3.2 Blasting fractures

The explosives are used to break the rock mass in conventional mining. Blasting the explosives inside the shot holes creates shock waves that fracture the rock mass. In a strong, brittle rock mass, the shock waves propagate more into the hangingwall and footwall. This is the case on the quartzite footwall zone, where both the hangingwall and footwall are strong and brittle and therefore more fractured. Blasting discipline is therefore very critical in the western part of the mine to limit the hangingwall damage.

5.4 Chapter Summary

The analysis of the results in this chapter has shown that the rock mass strength of the lava hangingwall is consistent throughout the mine. This suggests that the resultant damage is independent of the hangingwall strength but rather dependent on the footwall. The quartzite and the shale have significantly different intact and rock mass strengths. From the results above, we can conclude that softer Booysen's shale absorbs more strain energy during static and dynamic loading than the quartzite zones. The shale is more prone to creep, allowing closure and reducing fracturing in the hangingwall. Though there was an observed difference between the Elsburg/Danny's and Kimberley quartzite, the difference was insignificant and does not show significantly different behaviour.

Map3D elastic numerical modelling software showed a higher convergence and ERR in the shale. This was in line with expectations and observations. The quartzite material fractures more easily, generating smaller magnitude events. Fractures are expected to develop deeper in the face in the shale zone because of the ductile nature and creep of the shale material. The greater depth behind the face also suggests higher confinement and fewer fractures. The highly fractured rock in the quartzite zone suffers greater shakedown damage during the vibrations caused by a seismic event.

The brittle nature of the footwall rock formation results in a fractured rock mass. The blasting energy also contributes to opening the existing fractures around the stopes. The soft footwall conditions have fewer existing fractures for the blast gases to penetrate. The highly fractured conditions in the west tend to fail more easily between support units than in the east.

6 CONCLUSIONS AND RECOMMENDATIONS

6.1 Introduction

The study has shown clear differences between the shale and quartzite footwall areas in the mine. Ground control districts can be defined by the Booysens shale and Kimberley or Elsburg/Denny's quartzite footwall areas in the eastern and western parts of the mine, respectively. Differences have been identified in the physical conditions of the stopes, closure rates, seismic responses, and rock strength properties.

6.2 Summary of Chapters

This report has presented six chapters that cover the introduction, literature review, research approach, data for the study, analysis and findings, then conclusion and recommendations. The introduction chapter introduced the research background and context, then defined the problem statement and justified the need for the research. The research objectives were laid out, and the methods of research were explained. The sources of the data are explained, as well as the research validation process.

In the literature review chapter, the key concepts, theories and studies were defined. The first step was to define the lithology of the Witwatersrand basin and the lithologies found at Mponeng Mine. The challenges with each lithology were defined, and assumptions were drawn. The subject of seismicity and rockbursts was explored, and the sources of seismicity were defined. The concept of ERR was defined, and it is dependent on the stope convergence. The factors that influence convergence were explored. The study demonstrated how the intact rock strength was used to determine the rock mass strength. The chapter explained the key debates and controversies from previous studies at Mponeng Mine on the hard lava.

The research approach chapter defined the design of the research, highlighting the differences between the east and west parts of Mponeng Mine. The difference in the physical conditions between the east (Booysens Shale footwall) and the west

(quartzite footwall) geotechnical zones was clearly defined. The data validation steps were defined. The approach was to correlate the observed physical conditions to rock properties and seismic data.

In the data for the study chapter, the intact test results from the rock samples taken from each footwall zone were presented. Raise lines were strategically chosen for physical observations, and seismic data were described from each of the two main, defined ground control districts/zones. Ground conditions were found to be significantly better in the shale footwall than in the quartzite areas. Footwall heave was observed in the shale stopes, which corresponded with a higher closure rate. The observations correlated with the comparatively weaker and more ductile material shown by the laboratory tests.

The analysis of the results was provided in Chapter 5. It showed that the rock mass strength of the lava hangingwall was consistent throughout the mine. This suggests that the resultant damage was independent of the hangingwall strength but rather dependent on the strength properties of the footwall. The quartzite and the shale have significant differences in terms of intact rock strength and post-failure behaviour. The Elsburg/Danny's quartzite and Kimberley quartzite were similar and could, therefore, be considered a single ground control district.

The laboratory tests corresponded well with the underground observations. Even though the shale district had a higher ERR, there was significantly less damage reported for this area after a seismic event than for the quartzite district. This phenomenon could be explained by the observed fracturing, which was significantly less in the hangingwall of the shale district. The higher ERR in the shale district resulted from the creep behaviour of the shale. The lab tests proved that shale is more ductile than the hangingwall lava and quartzite. The East Mine system is much softer than the West Mine. It is thought that the shale deformation near the face may have reduced the hangingwall fracturing in this area, which would have transferred the high stress deeper into the face. Under such conditions, the confinement would also be higher and the fractures spaced further apart.

The quartzite footwall was able to fracture more easily, generating smaller magnitude events. The lower Poisson's ratio and high Young's modulus proved

that the quartzite was a brittle rock mass. Since the hangingwall lava has the highest Young's modulus, it made the whole system at the West Mine a stiff system. This resulted in fractures developing and propagating further into the hangingwall and footwall. The brittle and highly fractured rock mass failed more easily during the dynamic loading caused by a seismic event.

The blasting energy also contributes to the ground conditions. In the highly fractured quartzite zone, blast gases can open the existing fractures, making them loose and vulnerable to FOGs. The highly fractured conditions in the West Mine tend to fail more easily between support units than in the east. The softer system in the East Mine has fewer fractures; therefore, the blasting does not affect the ground conditions significantly. The ground remains stable and not vulnerable during a seismic event.

6.3 Research Observations

The research has shown that the effects of different rock properties between the East and West Mine are visible. The seismic response, magnitude distribution and rock mass response are variable between the two defined areas.

6.3.1 Initial and complementary studies

Multiple studies were conducted previously to understand the behaviour and sources of seismic events. Scheepers et al. (2012) conducted several studies to understand the effects of seismicity at Mponeng Mine. These studies correlated seismicity to the rate and volume of mining. The effects of the rock properties were not considered during the studies. The mining layouts were reviewed, and dip pillars were introduced to limit spans and effective closure; however, the study was not based on each geotechnical zone. Milev and Spottiswoode (2002) also studied the effects of rock properties on mining-induced seismicity in the Witwatersrand Gold Mines, including Mponeng Mine. Their studies concluded that the seismicity generated in the hard lava and hard quartzite footwall at the west side of the mine was not different to the seismicity generated in the hard lava and soft Booysen Shale footwall on the east side of the mine.

6.3.2 Key findings and observations

This study showed that the difference in rock properties between the east and west of Mponeng Mine affected the mining-induced seismicity. It also suggested that rock properties play a vital role in the rock mass behaviour and should be considered during the layout and support design process.

6.4 Research Contributions

This research will form an important part of the future mine layout and support design process at Mponeng Mine. There is an opportunity to maximise the mining layouts and limit the loss of ground, which currently happens towards the end of a raise line, where the last panels do not mine to the dip pillar limit. The support system must be designed for specific conditions.

Based on the results from this research, it is evident that there is less rock mass fracturing and damage in the Booysendal Shale geotechnical zone. The high Poisson's ratio of the shale footwall indicates the high yield capability, which helps to absorb the strain energy generated during the dynamic loading caused by the seismic events. This should allow the support standards to have a lower support resistance in this geotechnical zone than in the Quartzite footwall zone. However, the high closure rate will require the support units to have a higher yielding range. The lower face stresses may allow for a comparatively higher mining span, which can be achieved by reducing the frequency of strike pillars and thereby increasing the extraction ratio. This concept needs to be verified with measurements.

The support resistance in the quartzite geotechnical zone will need to be greater than in the shale footwall. Both areas will need to cater for energy absorption. The total spans may need to be comparatively less in the quartzite geotechnical zone due to the high face stresses. The study results have shown that there is a significant ore loss when the last panels in the profile are not in line with the leading panels on the dip pillar position. The stope design in this geotechnical zone should consider the high stress ahead of the panels and the high volume of damage during dynamic loading.

6.5 Research Limitations

The research did not consider the effects of mining rates and mining volumes; however, the previous studies conducted by Scheepers et al. (2012) have already considered these. The study areas were chosen to eliminate the variables; however, there were still some variables between the two areas that could not be eliminated, e.g. the large dykes east of the 116/65 raise line. The influence of the geological structures could not be quantified. It was, however, assumed to be insignificant due to the 20 m wide bracket pillars.

The source parameters of the events were not explored in this research; however, the slip-type events were removed. By eliminating the slip-type events, the West Mine (Quartzite Footwall) had more events than the East Mine (Shale Footwall). The events at the West Mine were, however, of smaller magnitude.

6.6 Recommendations for Future Research Work

The study has shown a difference between the rock mass response in the shale footwall and the rock mass response in the quartzite footwall. The study only focused on two representative raise lines to highlight the differences between the entire geographical area. The mine is currently not divided according to the geotechnical or footwall zones; it is, however, divided in the middle, which means that the historically recorded data for the East and West Mines doesn't represent the data of the shale footwall and quartzite footwall. It is recommended that:

- Data will be captured for each geotechnical zone, not just east and west.
- The source mechanism of events should be considered when reporting and gathering data, as it plays a significant role in the two areas.
- The support system should be specific for each geotechnical zone based on the prevailing conditions. Closer support spacing is required in the quartzite footwall due to the highly fractured nature of the rock mass, and wider support spacing in the shale footwall due to more competent ground conditions.
- The mining span and stope geometry must be designed for each footwall zone, considering the seismic response and the rockburst data. The burst-

type events increase as the panels mine in line along the dip pillar. There is a need to consider profiling the dip pillars, especially in the quartzite footwall zone.

- The impact of different lead/lag distances and panel lengths in each footwall zone should be investigated as part of the future studies.
- The effect of changing the profile should be investigated for each area.

REFERENCE LIST

Armaghani, D.J., Mohamad, E.T., Momeni, E., Narayanasamy, M.S., Amin, M.F.M., 2015. *An Adaptive Neuro-fuzzy Inference System for Predicting Unconfined Compressive Strength and Young's Modulus: A Study on Main Range Granite. Bulletin of Engineering Geology and Environment*. 74, pp. 1301–1319. [Online]
Available at: https://doi.org/10.1007/s10064-014-0687-4
[Accessed June 2024]

Bieniawski, Z.T., 1974. *Estimating the Strength of Rock Materials*. Journal of the Southern African Institute of Mining and Metallurgy. 8, pp. 312–320.

Bieniawski, Z.T., Hawkes, I., 1978. *Suggested Method for Determining Tensile Strength of Rock Materials*. International Journal of Rock Mechanics and Mining Sciences & Geomechanics Abstracts. Pergamon Press Ltd, Great Britain. 15, pp. 99–103.

Bonini, M., Debernardi, D., Barla, M., Barla, G., 2007. *The Mechanical Behaviour of Clay Shales and Implications on the Design of Tunnels.* Rock Mechanics and Rock Engineering. 42, pp. 361–388. [Online]
Available at: https://doi.org/10.1007/s00603-007-0147-6
[Accessed June 2024]

Brady, B.H.G., Brown, E.T., 2004. *Rock Mechanics for Underground Mining*, 3rd ed. Springer, Dordrecht, The Netherlands.

Chang, C., Zoback, M.D., Khaksar, A., 2006. *Empirical Relations Between Rock Strength and Physical Properties in Sedimentary Rocks.* Journal of Petroleum Science and Engineering. 51, pp. 223-237

Daehnke, A., van Zyl, M., Roberts, M.K.C., 2001. *Review and Application of Stope Support Design Criteria.* The Journal of South African Institute of Mining and Metallurgy, pp. 135-164

de Kock, W.P., 1940. *The Ventersdorp Contact Reef. Its Nature, Mode of Occurrence and Economic Significance. With Special Reference to the Far West Rand.* South African Journal of Geology, 43, pp. 85–107.

Drescher, K., Handley, M.F., 2003. *Aspects of Time-dependent Deformation in Hard Rock at Great Depth.* Journal of the Southern African Institute of Mining and Metallurgy. 103 (5), pp. 325–336.

Duraprai, S., 2015. *An Investigation of Westonaria Formation Lavas (WAF) and its Influence on the Rock Engineering Design at Goldfields No. 4 (Ya Rona) Shaft Pillar Extraction.* MSc research report, University of Witwatersrand, Johannesburg.

Durrheim, R.J., 2010, *'Mitigating the Risk of Rockbursts in the Deep Hard Rock Mines of South Africa: 100 years of research'*, in J Brune (ed), Extracting the Science: a Century of Mining Research, Society for Mining, Metallurgy, and Exploration, Inc., Englewood, pp. 156-171

Durrheim, R.J., Anderson, R.L., Cichowicz, A., Ebrahim-Trollope, R., Hubert, G., Kijko, A., McGarr, A., Ortlepp, W.D., van der Merwe, N., 2006. *The Risks to Miners, Mines, and the Public Posed by Large Seismic Events in the Gold Mining Districts of South Africa.* In Proceedings of the Third International Seminar on Deep and High Stress Mining, 2-4 October 2006, Quebec City, CANADA, J Hadjigeorgiou and M Grenon (editors), Universitè Laval, Canada.

Durrheim, R.J., Roberts, M.K.C., Haile, A.T., Hagan, T.O., Jager, A.J., Handley, M.F., Spottiswoode, S.M., Ortlepp, W.D., 1998. *Factors Influencing the Severity of Rockburst Damage in South African Gold Mines.* Journal of the Southern African Institute of Mining and Metallurgy. 2. pp. 53–58.

Ghosh Roy, M., Rao, K.S., 2015. *Analysis of Creep Behaviour of Soft Rocks in Tunnelling.* Presented at the India Society of Engineering Geology-Engineering Geology in New Millennium, New Delhi.

Grove, D., 2006. T*he Effect of Different Lava Lithologies on Hangingwall Ground Conditions at Mponeng Mine.* Mponeng Mine presentation.

Hagan, T.O., 1981. *Micro-seismic Events: An Aid in Studies of Deep-mine Rock Structures*. Journal of the South African Institute of Mining and Metallurgy, 11, pp. 319-320

Hoek, E., 1994. *Strength of Rock and Rock Masses.* International Society of Rock Mechanics News Journal. 2, pp. 4–16.

Hoek, E., Brown, E.T., 2018. *The Hoek-Brown Failure Criterion and GSI* - 2018 edition. Journal of Rock Mechanics and Geotechnical Engineering, 11, pp. 445–463.

Hoek, E., Brown, E.T., 1997. *Practical Estimates of rock mass strength.* International Journal of Rock Mechanics and Mining Sciences. 34, pp. 1165–1186.

Hoek, E., Brown, E.T., 1980a. *Empirical Strength Criterion for Rock Masses.* ASCE Journal of the Geotechnical Engineering Division. 106 (9), pp. 1013–1035.

Hoek, E., Brown, E.T., 1980b. *Underground Excavations in Rock.* The Institute of Mining and Metallurgy, London.

Hoek, E., Martin, C.D., 2014. *Fracture Initiation and Propagation in Intact Rock – A review.* Journal of Rock Mechanics and Geotechnical Engineering, 6, 287–300. [Online]
Available at: https://doi.org/10.1016/j.jrmge.2014.06.001
[Accessed January 2024]

Hofman, G., 2012. *Correlating Modelled Elastic Energy Release with Recorded Seismicity in a Deep Tabular Mine.* The Southern African Institute of Mining and Metallurgy. Conference: Southern Hemisphere International Rock Mechanics Symposium SHIRMS 2012. In South Africa, S71

Jager, A.J., Ryder, J.A., 1999. *A handbook on Rock Engineering Practice for Tabular Hard Rock Mines.* SIMRAC, Johannesburg.

Kahraman, S., Fener, M., Kozman, E., 2012. *Predicting the Compressive and Tensile Strength of Rocks from Indentation Hardness Index.* Journal of the Southern African Institute of Mining and Metallurgy. 112, pp. 331–339.

Kaiser, P.K., Cai, M., 2013. *Keynote Lecture: Rockburst Damage Mechanisms and Support Design Principles.* 8th Int. Symp. Rockburst Seism. Mines Malovichko Malovichko Eds GS RAS MI UB RAS Obninsk-Perm, ISBN 978-5-903258-28-4, pp. 349–370.

Kaiser, P.K., Cai, M., 2012. *Design of Rock Support System Under Rockburst Condition*. Journal of Rock Mechanics and Geotechnical Engineering. 4 (3), pp. 215–227 [Online]
Available at:
https://pdfs.semanticscholar.org/0ffb/514738e674ce522060bcffce29ea79283a31.pdf
[Accessed August 2025]

Labuz, J.F., Zang, A., 2012. *Mohr-Coulomb Failure Criterion.* Rock Mechanics and Rock Engineering, 45, pp. 975–979. [Online]
Available at: https://doi.org/10.1007/s00603-012-0281-7
[Accessed June 2024]

Malan, D.F., Napier, J.A.L., n.d. *Rockburst Support in Shallow-dipping Tabular Stopes at Great Depth.* Department of Mining Engineering, University of Pretoria, South Africa [Online]
Available at:
https://repository.up.ac.za/server/api/core/bitstreams/43917d36-85ba-4cd9-8713-224428b6bd35/content [Accessed August 2025]

McGill, R.B., Russo-Bello, F.D., Kershaw, D.J., Laas, J.J., 2023. *Mponeng Mine Mandatory Code of Practice to Combat Rockfall and Rockburst Accidents in Tabular Metalliferous Mines.* WA_COP_GEN_001. Revision 10, pp. 36-44

Milev, A.M., Spottiswoode, S.M., 2002. *Effect of the Rock Properties on Mining-induced Seismicity Around the Ventersdorp Contact Reef, Witwatersrand Basi, South Africa.* Pure and Applied Geophysics 159, 165-177

Modisha, S., Zvarivadza, T., 2015. A *Review of Preconditioning and its Influence on Mining Conditions with Particular Emphasis on Health and Safety.* 24th International Mining Congress and Exhibition of Turkey (IMCET 2015) Antalya, Turkey, pp. 113-122 [Online]
Available at: https://www.proceedings.com/content/026/026166webtoc.pdf [Accessed August 2025]

Nyungu, D., Stacey, T.R., 2014. *Time-dependent Tensile Strengths of Bushveld Complex Rocks and Implications for Rock Failure Around Mining Excavations,* Journal of the Southern African Institute of Mining and Metallurgy, 114 (10), pp. 8.

Ozturk, C.A., Nasuf, E., Kahraman, S., 2014. *Estimation of Rock Strength from Quantitative Assessment of Rock Texture.* Journal of the Southern African Institute of Mining and Metallurgy,114(6), pp. 10.

Palmstrom, A., Broch, E., 2006. *Use and Misuse of Rock Mass Classification Systems with Particular Reference to the Q-system.* Tunnelling and Underground Space Technology. 21 (6), pp. 575–593.

Rakumakoe, O., 2019. *Ideal Stope Profile to Manage Seismicity in Deep Tabular Narrow Reef Mines,* in W. Joughin (ed.), Deep Mining 2019: Proceedings of the Ninth International Conference on Deep and High Stress Mining, The Southern African Institute of Mining and Metallurgy, Johannesburg, pp. 293-306 [Online]
Available at: https://doi.org/10.36487/ACG_rep/1952_22_Rakumakoe [Accessed August 2025]

Reimold, W.U., Viljoen, M.J., 1994. *Special Issue on the Ventersdorp Contact Reef.* South African Journal of Geology, 97, pp. 234–237.

Richardson, P., van Helten, J.J., 1984. T*he Development of the South African Gold-Mining Industry, 1895-1918.* The Economic History Review. 37 (3), pp. 319–340. [Online]
Available at: https://doi.org/10.2307/2597284
[Accessed March 2024]

Roberts, M.K., Schweitzer, J.K., 1999. *Geotechnical Areas Associated with the Ventersdorp Contact Reef*. Witwatersrand Basin, South Africa, pp. 157–166.

Ryder, J.A., Jager, A.J., 2002. *A Textbook on Rock Mechanics for Tabular Hard Rock Mines.* The safety in Mines Research Advisory Committee (SIMRAC), Johannesburg.

Scheepers, L.J., Hofmann, G., Morkel, I.G., 2012. *The Study of Seismic Response to Production for a Grid Mining Layout.* The South African Institute of Mining and Metallurgy, Southern Hemisphere International Rock Mechanics Symposium SHIRMS, pp. 387–406.

Singh, B., Goel, R.K., 2011. *Engineering Rock Mass Classification: Tunneling, Foundations, and Landslides.* Butterworth-Heinemann.

Thebethe, Z., 2018. *Assessing Preconditioning Effectiveness Using Ground Penetrating Radar Mapping.* MSc research report, University of Witwatersrand, Johannesburg. [Online]
Available at: https://wiredspace.wits.ac.za/items/3951b4c7-5598-47a6-9240-3a67eb47249a
[Accessed August 2025]

Ulusay, R. and Hudson, J.A., 2007. *Laboratory Testing. The Complete ISRM Suggested Methods for Rock Characterization, Testing and Monitoring: 1974-2006.* Suggested Methods Prepared by the Commission on Testing Methods, International Society for Rock Mechanics, Compilation Arranged by the ISRM Turkish National Group, Ankara, Turkey, ISBN 978-975-93675-4-1, pp. 157-184

Winter, H.R., 1976. *A Lithostratigraphic Classification of the Ventersdorp Succession.* Transvaal Geology Society of South Africa. 79, 31–48.

Wong, I.G., 1992. *Recent Developments in Rockburst and Mine Seismicity Research,* in: 33rd U.S. Symposium. Presented at the Rock Mechanics, J.R. Tillerson & W.R. Wawersik (eds), A. A. Balkema Publishers, Santa Fe, New Mexico, pp.1103–1112.

Ye, Y., Tang, S., Xi, Z., Lu, R., Zhang, Z., Li, J., 2024. *The Effects of Quartz Content, Particle Size and Distribution Mode on the Mechanical Properties and Fracturing of Shale.* Natural Resources Research. 33, pp. 239–262. [Online]
Available at: https://doi.org/10.1007/s11053-023-10267-4
[Accessed August 2024]

Zhang, D., Ranjith, P.G., Perera, M.S.A., 2016. *The Brittleness Indices Used in Rock Mechanics and their Application in Shale Hydraulic: A Review.* Journal of Petroleum Science and Engineering. 143, pp. 158-170 [Online]
Available at: www.elsevier.com/locate/petrol
[Accessed January 2024]

APPENDIX A. TABLE OF LABORATORY UNI-COMPRESSIVE STRENGTH WITH MODULUS TESTS RESULT

Appendix Table 1: UCM results for the hangingwall and footwall core samples taken from the three footwall zones found at Mponeng Mine

Uniaxial Compressive Strength (UCS), Elastic Modulus (E), Poisson's Ratio (ν)											
Rock Type	**Specimen Ref No**	**Diameter (mm)**	**Length (mm)**	**L/D**	**Mass (g)**	**Density (kg/m3)**	**Failure Load (kN)**	**UCS (MPa)**	**E (GPa)**	**ν**	**Test Type**
Mponeneg East Booysens Shale Footwall Zone											
Booysens Shale	1	41.95	104.70	2.5	397.3	2745	216.7	**156.8**	65.05	0.27	UCM
	2	41.70	104.60	2.5	395.3	2767	213.9	**156.6**	61.78	0.33	UCM
	3	41.90	106.20	2.5	401.3	2740	267.6	**194.0**	69.35	0.26	UCM
	4	41.80	104.50	2.5	394.3	2750	266.7	**194.3**	60.46	0.23	UCM
	5	42.00	104.65	2.5	398.6	2749	222.9	**160.9**	64.65	0.27	UCM
Lava	1	41.90	106.10	2.5	412.6	2820	279.4	**202.6**	83.38	0.27	UCM
	2	42.00	106.20	2.5	422.5	2872	465.8	**336.2**	92.50	0.22	UCM
	3	42.00	106.10	2.5	416.5	2833	363.1	**262.1**	86.09	0.23	UCM
	4	41.90	106.40	2.5	413.1	2816	399.9	**290.0**	81.86	0.26	UCM
	5*	41.90	106.30	2.5	426.4	2909	170.9	**123.9**	97.10	0.25	UCM
Mponeneg Middle - West Kimberly Quartzite Footwall Zone											
Kimberley Quartzite	1	42.00	105.40	2.5	388.1	2658	360.0	**259.9**	79.05	0.19	UCM
	2	42.00	105.00	2.5	386.3	2656	447.0	**322.7**	81.31	0.11	UCM
	3	42.00	104.90	2.5	386.9	2662	460.2	**332.2**	82.02	0.13	UCM
	4	42.00	104.20	2.5	383.7	2658	447.8	**323.2**	80.97	0.09	UCM
	5	42.00	104.80	2.5	388.0	2672	375.3	**270.9**	76.02	0.16	UCM
Lava	1	42.00	104.20	2.5	412.3	2856	418.1	**301.8**	85.12	0.27	UCM
	2	41.90	104.80	2.5	415.1	2873	460.3	**333.8**	87.28	0.21	UCM
	3	41.80	104.70	2.5	401.2	2792	292.0	**212.8**	72.41	0.27	UCM
	4	41.90	104.00	2.5	401.0	2796	278.2	**201.8**	77.96	0.24	UCM
	5	42.00	104.00	2.5	404.7	2809	389.5	**281.2**	83.59	0.27	UCM
Mponeneg Far West Elsburg Footwall Zone											
Elsburg Quartzite	1	31.60	87.90	2.8	184.2	2672	134.6	**171.6**	74.52	0.18	UCM
	2	31.60	88.00	2.8	184.4	2672	151.3	**192.9**	75.39	0.16	UCM
	3	31.60	88.00	2.8	184.7	2676	176.2	**224.6**	74.43	0.20	UCM
	4	32.00	88.00	2.8	188.2	2659	212.3	**264.0**	75.72	0.17	UCM
	5	31.60	88.00	2.8	185.2	2683	125.1	**159.5**	72.16	0.16	UCM
Lava	1	32.00	88.50	2.8	203.00	2852	187.87	**233.6**	77.43	0.24	UCM
	2	32.00	88.40	2.8	200.90	2826	217.70	**270.7**	78.48	0.22	UCM
	3	32.00	88.50	2.8	201.60	2832	177.04	**220.1**	77.08	0.22	UCM
	4	31.90	88.50	2.8	204.8	2895	215.0	**269.0**	88.42	0.22	UCM
	5	32.00	88.40	2.8	206.1	2899	296.1	**368.2**	89.53	0.25	UCM
* : Failed along a pre-existing crack											